Estimating the Influence of Sea Level Rise and Climate Change on Storm Surges in Western Taiwan

Yuchia Chang [1], Martin Mäll[2], Ryota Nakamura [3], Tomoyuki Takabatake [4], Jeremy Bricker [5], Miguel Esteban [6], Tomoya Shibayama [7]

Abstract

Situated in the Western Pacific Ocean, Taiwan is frequently affected by powerful typhoons. The present research evaluates the storm surges that could take place along the western coastline of Taiwan, and the design water level that will likely be required by adaptation countermeasures in the course of the 21st century to protect coastal settlements. To do so, the intensity of a given case study typhoon (Soudelor, which caused great damage to Taiwan in 2015) that could affect the target case study area (Yunlin county) was modified by taking into account climate change and sea level rise by changing the sea surface temperature, atmospheric air temperature, and relative humidity expected in the year 2041~2060 and 2081~2100 time horizons. The Advanced Research Weather Research and Forecasting Model (WRF-ARW) and the Unstructured Finite Volume Community Ocean Model (FVCOM) were utilized to simulate the typhoons and storm surges. The hindcasting of the historical typhoon showed good agreement with the observed data provided by the Central Weather Bureau (CWB) in Taiwan, and the simulations under future climate change scenarios forecasted an increase in typhoon intensity, especially the maximum wind speed. However, the storm surge simulations indicated a limited increase in storm surge height, and even a decrease when considering also SLR. Nevertheless, the estimated maximum water level, including both the effect of SLR and future storm surge height, can increase up to 3.53 m and 3.84 m relative to mean sea level at the tidal stations in Yunlin and Chiayi County, respectively. The results showed that storm surges in the study area, characterized by a shallow bathymetry with many sandbars and land reclamation projects, are highly influenced by the change in water depth due to SLR and tidal changes, and the existence of the Central Mountain Range, which can greatly affect the accuracy of the simulated typhoon wind fields.

[1]joe85122280234@gmail.com, Waseda University, Tokyo, Japan
[2]mallmartin4@gmail.com, Yokohama National University, Yokohama, Japan
[3]r-nakamura@eng.niigata-u.ac.jp, Niigata University, Niigara, Japan
[4]takabatake@civileng.kindai.ac.jp, Kindai University, Osaka, Japan
[5]jeremydb@umich.edu, University of Michigan, Ann Arbor, USA
[6]esteban.fagan@gmail.com, Waseda University, Tokyo, Japan
[7]shibayama@waseda.jp. Waseda University, Tokyo, Japan

Keywords

Typhoons, Climate change, Storm surges, Taiwan

1   Introduction

Taiwan is an island located at the western side of the Pacific Ocean that is frequently affected by typhoons between the months of July and September (Liu et al., 2018), which can cause devastating damage to the various settlements situated along its coastline. According to the Central Weather Bureau (CWB) of Taiwan, the island has been affected by an average of 3 to 4 typhoons each year. Furthermore, the island is located on one of the convergent plate boundaries that surround the Pacific Ocean, meaning that around 46.5% of it is made of mountainous areas (Directorate-General of Budget, Accounting and Statistics, 2020). Such relief exacerbates the heavy rain that takes place during the passage of typhoons, resulting in frequent flooding to the downstream areas of rivers. Aside from fluvial flood risks, typhoons also pose a considerable risk to coastal communities due to the storm surges they can generate.

Most of the storm surges in Taiwan that have exceeded 1 m since 1958 were recorded along the northern coastline of the country, mainly caused by "northwestern typhoons" (Yang et al., 2018). This term indicates a type of typhoon that approaches the island from the east and then circumvents the north coast without making a landfall, with winds and heavy rain arriving from the northwest, and often resulting in saltwater intrusion (Ministry of Culture, 2009). However, even though storm surges in Southern Taiwan are seldom higher than 1 m, this nevertheless can sometimes represent 80% of the average tidal range[1], which is much higher than the 40% to 50% of the average tidal range in Northern and Central Taiwan, making the area more vulnerable to storm surges (Yang et al., 2018).

The Advanced Research Weather Research and Forecasting Model (WRF-ARW) (Skamarock et al., 2008) has been widely applied to simulate mesoscale weather systems, including the forecasting of typhoons and the hindcasting of historical cases. For the case of Taiwan, Typhoon WRF (TWRF) has been in operational use since 2010, aiming to provide more accurate simulations for typhoons over East Asia using a regional high-resolution model. Although it has been pointed out by Hsiao et al. (2020) that the model still has some disadvantages compared to other models that can simulate tropical cyclone related heavy rainfall using moving nested meshes, it shows that one of the key problems for accurately simulating typhoons over Taiwan is the complicated mountainous nature of the terrain. Essentially, typhoon track and intensity simulations can be rather inaccurate due to the existence of the Central Mountain Range (a high mountain range that traverses Taiwan from north to south), since these simulations are very sensitive to sudden orographic changes (Hsiao et al., 2020).

Despite the efforts that have been made in Taiwan to accurately reproduce the passage of typhoons and the rainfall that accompanies them, the simulation of storm surges based on meteorological data has received comparatively little attention. Instead, much of the research on storm surges in the country has utilized data analysis methods to predict future storm surge heights based on historical records (Yang et al., 2018, Chang et al., 2004, Chang, 2008). Yang et al. (2018) reviewed storm surges in Taiwan from 1958 to 2017 and arrived at the conclusion that, although such phenomena were low in height compared to other countries, they can still be destructive due to the characteristics of the coastal areas and the design criteria employed (whereas the 50 year return storm surge height might be higher than the level of coastal dykes in some areas). Nevertheless, some research has been conducted in recent years to study the effect of storm surges in Taiwan utilizing a variety of methods, with one common approach being the combined use of the Simulating Waves Nearshore (SWAN) model and the ADvanced CIRCulation (ADCIRC) model. Yu et al. (2019) assessed the potential highest storm surge tide using this coupled model by evaluating the highest storm surges and highest astronomical tides. A hazard map was then plotted by categorizing the hazard level based on its results. Liu & Huang (2020) also used this model to attempt to understand the physical factors that dominate storm surge heights during the passage of typhoons in Taiwan. However, the use of a wider variety of models is warranted, in order to obtain a better picture of how storm surges are generated in the country, especially around the western coast. Particularly, given the challenge that climate change represents for coastal areas, is important to further the understanding of potential storm surge impacts under climate change induced environmental changes (including both changes in atmospheric and water temperatures, and sea level rise).

Most work related to weather extremes and climate change study the output from general circulation models (GCMs; e.g. Zappa et al., 2013)) to find common signals and trends in potential future changes (e.g. frequency, intensity and track shifts). However, few studies have focused on the direct effect of individual parameters, such as sea surface temperature

---

[1] The tidal range is in the order of 1 m.

(SST) and atmospheric air temperature (AAT) on the intensity of tropical cyclones and associated storm surges. The method to study individual atmospheric events under changing background future conditions is known as the pseudo-global-warming method (Schär et al., 1996; Sato et al., 2007). For tropical cyclones this method has been applied by Nakamura et al. (2016; 2020), who studied the super Typhoon Haiyan in 2013 by considering the influence of SST, AAT, and relative humidity (RH) to simulate future scenarios (under the CMIP5 framework). While they conclude that the intensity of typhoons should increase under future climate conditions, they also noted the dampening influence caused by changes in AAT, probably due to reduced latent and sensible heat fluxes and decreased cyclone convection (Wang et al. 2014). However, it would appear that it is difficult to generalize and obtain definite conclusions regarding the direct effect of individual atmospheric and oceanic parameters on the intensity of future typhoons, given the few case studies that have been analysed until present.

The aim of this paper is thus to understand the effect that potential changes in typhoon intensity due to climate change and sea level rise could have on storm surges on the west coast of Taiwan (particularly in areas that are below mean water level due to rapid levels of land subsidence). To do so, the authors first validated WRF and the Unstructured Finite Volume Community Ocean Model (FVCOM) by hindcasting Typhoon Soudelor in 2015. The future conditions in the area were then simulated to understand the likely intensification of future typhoons in the Western Pacific Ocean due to higher sea surface temperatures (SST). To do so, the CMIP5 GCMs were utilized, considering also a variety of different likely SLR scenarios.

2   Study area and target typhoon

The study area of this research is Yunlin County, located on the western coastline of Taiwan (Figure 1 top), which is particularly at risk of flooding due to either coastal surges or riverine floods. The county also faces the Taiwan Strait, a relatively shallow sea with an average depth of only around 100 meters, as shown in Figure 1 bottom (Ministry of Culture, 2009).

Yunlin County has long been famous for its agricultural produce, though in the 1970s the price of farm products began to drop, and the potential of aquaculture started to be noticed by local residents. With the increased demand for freshwater, and due to insufficient surface water supply, groundwater extraction started to be widely utilized in the area, which in turn resulted in land subsidence. According to measurements by the Taiwanese government, the coastline area of Yunlin subsided by 2.2 meters between 1985 and 2019. Such severe land subsidence not only damaged the railway that runs through the district, but also increased the vulnerability of the area to storm surges and increased river discharge during the passage of typhoons (Information of Land Subsidence Prevention in Taiwan, 2020). As a result, coastal defences were built to prevent the area from being flooded (see Figure 2).

Typhoon Soudelor, one of the strongest typhoons of 2015 (Chang et al., 2015) is the target storm of the present study. It first formed as a tropical depression on July 29 and quickly gathered strength as it approached Taiwan (Figure 1a), making landfall on August 8 (04:40 AM Taiwan time). At the time of landfall it had maximum sustained winds of up to 173 km/h or 107 mph (more details can be found in Fakour et al. 2016). According to the emergency response report for this weather event, provided by the National Science and Technology Centre for Disaster Reduction in Taiwan (NCDR), the passage of the storm led to 8 deaths, 4 missing persons, 437 injured persons, and a total of 2.28 billion NTD in economic losses (~71.82 million USD; NCDR, 2015). Typhoon Soudelor (2015) was mainly chosen as a representative case study due to its relative recency and high impact along the Yunlin coastline. It is therefore desirable to further understand the potential impacts of such typhoon under future (warmer) climate conditions when also considering the effects of land subsidence in the area. For other localized impact studies different typhoon may be more suitable and representative cases should be selected accordingly (e.g. after Yu et al., 2019).
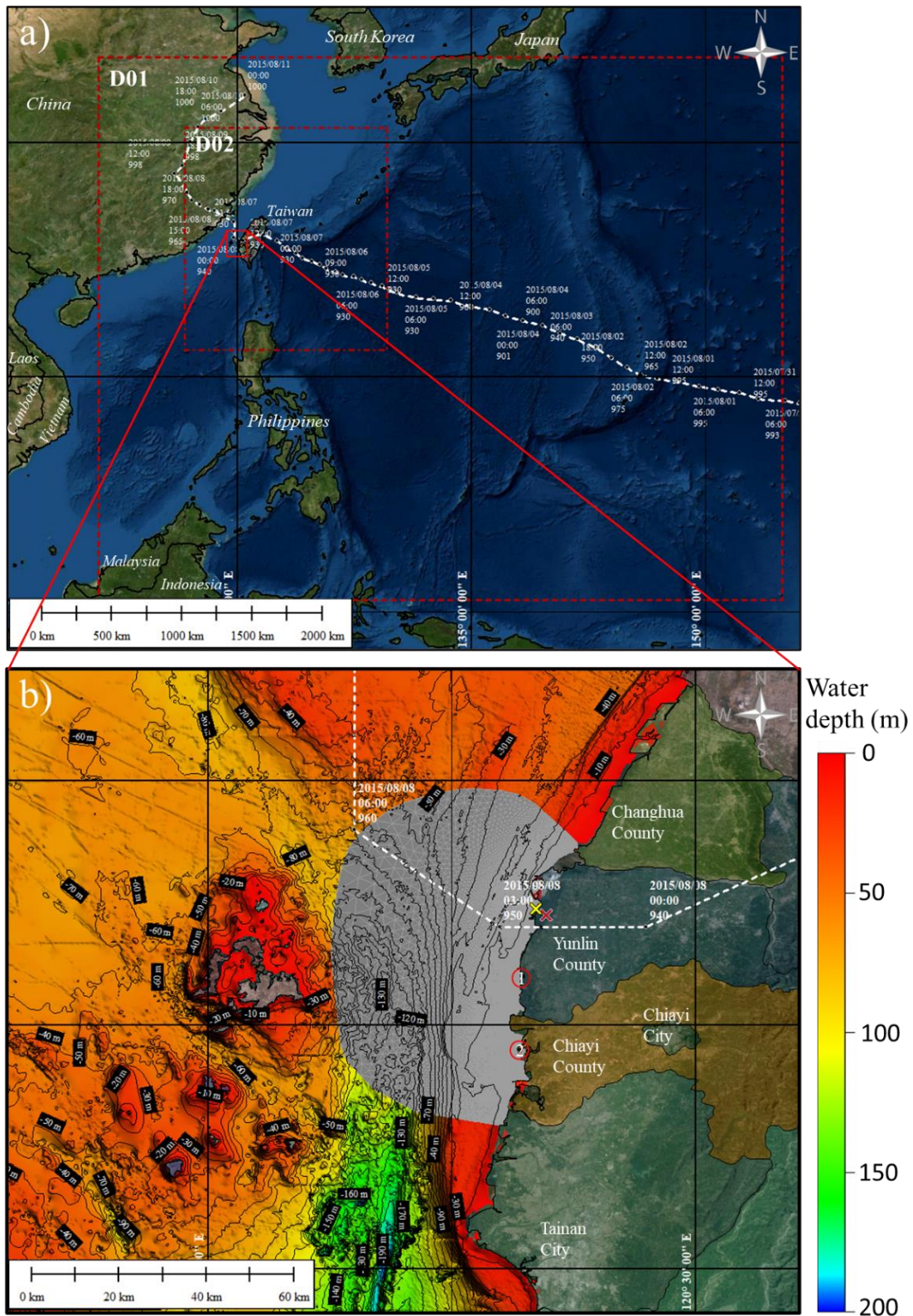
Figure 1: Study area and modelling setup, where a) shows the track of typhoon Soudelor (two upper lines are date and time, respectively; bottom line shows minimum seal level pressure). Dashed boxes D01 and D02 show the extent of the parent and second WRF modelling domains, respectively. Figure b) shows the main study area along the Yunlin and Chiayi Counties in Taiwan. The grey triangular mesh shows the unstructured modelling domain used in the FVCOM model. The circled numbers 1 and 2 show the Boziliao and Dongshi tidal stations, respectively. The yellow and red crosses on the Yunlin County coastline show the location of fish farms and coastal defensive structures, as shown on Figure 2, respectively. The bathymetry was built from the 200 m ODB data (same data used in FVCOM).

Figure 2: Left. Fish farms in Yunlin. Right. Coastal protection structures in Yunlin

3 Methodology

The methodology used by the authors to estimate storm surges is based on a combination of WRF and FVCOM, as shown in Figure 3. The WRF Preprocessing System (WPS) version 4.2 was used to generate the inputs for real-data simulations with the meteorological data provided by National Centre for Atmospheric Research (NCAR). The inputs were then applied in WRF-ARW version 4.2 to simulate the 2015 Typhoon Soudelor. For future scenarios, three parameters processed by WPS, namely SST, AAT, and RH were modified according to parameter changes within the selected CMIP5 GCMs. The wind and pressure data from WRF Domain 2 outputs were then extracted and used as inputs for FVCOM 4.1. The Taiwan Strait bathymetry data was provided by the Ocean Data Bank (ODB) of the Ministry of Science and Technology, Republic of China. The data was provided in a 200 m grid size and mostly collected by research vessels using single-beam echo sounder system since 1989, including few areas in which such data replaced by that
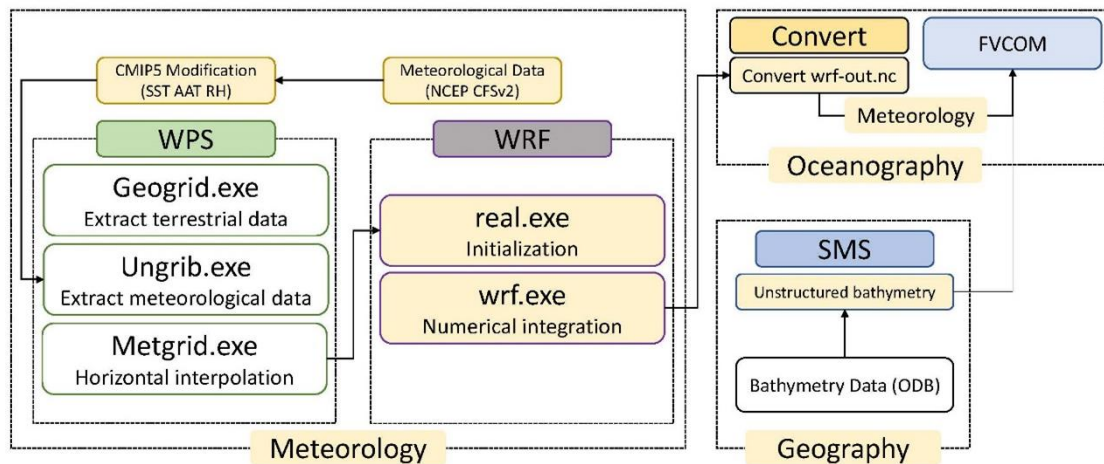

Figure 3: WRF-FVCOM Schematic Diagram

collected with a multi-beam echo sounder in survey EW9509 in 1995. The shape of the coastline was based on Shuttle Radar Topography Mission 3 arc-second (SRTM3) from the U.S. Geological Survey, with some modifications according to the bathymetry data obtained from the Ocean Data Bank (ODB). The modifications to the coastline and the construction of the mesh used in FVCOM simulations were done using the Surface-water Modelling System 13.0 (SMS).

3.1 Metocean simulations

The ARW used in this study is one of the two dynamics solvers in the WRF Software Framework (WSF), which is a collaborative work among the National Centre for Atmospheric Research (NCAR), the National Centres for Environmental Prediction (NCEP), and many other institutions (Skamarock et al., 2008). The meteorological data used for the WRF simulations were obtained from the Climate Forecast System Version 2 (CFSv2) 6-hourly products provided

by the NCEP. The initial atmospheric inputs for WRF included data with two different resolutions. The atmospheric pressure level had a resolution of $0.5° × 0.5°$, while the surface level and the flux fields level had a finer resolution of $0.2° × 0.2°$.

The physical parameters, schemes, and conditions used in the simulations are listed in Table 1, based on the studies performed by other researchers. For instance, the authors tested the settings used in TWRF that provided certain accuracy on simulating typhoons passing through Taiwan (Hsiao et al., 2020), in a study on Typhoon Morakot with a high-resolution initialization (Nguyen & Chen, 2011), and in the sensitivity study on precipitation forecast in Korea using one-way nesting in WRF (Jee & Kim, 2017). The conditions were then modified according to WRF sensitivity tests conducted by the authors to better reproduce the passage of typhoons around Taiwan. The three major aspects that were used to evaluate the accuracy of the simulation were the typhoon track, minimum sea-level pressure (MSLP), and maximum wind speed (MWS). When looking at these three aspects, the Purdue Lin microphysics scheme (Chen & Sun, 2002) provides the results closest to the observed parameters of the historical typhoon, with the other physics options tested having only a minor influence. The observed atmospheric data from several automatic meteorological observation stations maintained by Central Weather Bureau (CWB) of Taiwan were also compared with the model to evaluate the simulation accuracy. In the WRF simulations, two simulation domains were used, as shown in Figure 1. The FVCOM parameters used were based on studies by Nakamura et al. (2016, 2019, 2020) and Mäll et al. (2020).

This study used FVCOM version 4.1 (Chen et al., 2013) for the simulation of storm surges, which is a prognostic, unstructured grid, finite-volume, 3D primitive equation coastal ocean circulation model. The model is well known for its flexible unstructured grids that help better resolve coastal areas and estuaries with complex geometry. FVCOM, in the absence of ice and snow, consists of momentum, continuity, temperature, salinity, and density equations. It uses the finite-element method (FEM) to solve the following governing momentum equations by computing fluxes between non-overlapping horizontal triangular control volumes:

$$\frac{\partial u}{\partial t} + u\frac{\partial u}{\partial x} + v\frac{\partial u}{\partial y} + w\frac{\partial u}{\partial z} - fv = -\frac{1}{\rho_0}\frac{\partial(p_H + p_a)}{\partial x} - \frac{1}{\rho_0}\frac{\partial q}{\partial x} + \frac{\partial}{\partial z}\left(K_m\frac{\partial u}{\partial z}\right) + F_u \tag{1}$$

$$\frac{\partial v}{\partial t} + u\frac{\partial v}{\partial x} + v\frac{\partial v}{\partial y} + w\frac{\partial v}{\partial z} + fu = -\frac{1}{\rho_0}\frac{\partial(p_H + p_a)}{\partial y} - \frac{1}{\rho_0}\frac{\partial q}{\partial y} + \frac{\partial}{\partial z}\left(K_m\frac{\partial v}{\partial z}\right) + F_v \tag{2}$$

$$\frac{\partial w}{\partial t} + u\frac{\partial w}{\partial x} + v\frac{\partial w}{\partial y} + w\frac{\partial w}{\partial z} = -\frac{1}{\rho_0}\frac{\partial q}{\partial z} + \frac{\partial}{\partial z}\left(K_m\frac{\partial w}{\partial z}\right) + F_w \tag{3}$$

$$\frac{\partial u}{\partial x} + \frac{\partial v}{\partial y} + \frac{\partial w}{\partial z} = 0 \tag{4}$$

where x, y, and z are the east, north, and vertical axes in the Cartesian coordinate system; u, v, and w are the x, y, z velocity components; ρ is the density; p_a is the air pressure at sea surface; p_H is the hydrostatic pressure; q is the non-hydrostatic pressure; f is the Coriolis parameter; K_m is the vertical eddy viscosity coefficient. For the air-sea drag coefficient C_d, the authors used the values tested by Nakamura et al. (2016), which are based on Honda & Mitsuyasu (1980).

$$C_d = (1 - 0.01890 × W_S) × 0.00128 \quad if\ W_S \le 8\ ms^{-1} \tag{5}$$

$$C_d = (1 + 0.1078 × W_S) × 0.000581 \quad if\ 8\ ms^{-1} \le W_S \le 30\ ms^{-1} \tag{6}$$

$$C_d = 0.00246 \quad if\ W_S \ge 30\ ms^{-1} \tag{7}$$

where W_S is the wind velocity.

FVCOM simulations were performed using the WRF simulation results from Domain 2, with a simulation period from 00:00 UTC August 7 to 00:00 UTC August 9 (48 hours). The mesh size used in the simulation started from around 100 m along the coastline to a maximum of 5000 m at the furthest point from the coastline (at the open boundary, see supplementary information).

Table 1: Simulation condition setup ([ ] indicates the option number in WRF namelist)

WRF	
Domains	2
Domain grid size	Domain 1: 9 km; Domain 2: 3 km
Simulation time (Domain 1, 2)	00:00 UTC August 5, 2015 - 00:00 UTC August 11, 2015
Domain size (East-West)(grid numbers)	Domain 1: 470; Domain 2: 418
Domain size (South-North)(grid numbers)	Domain 1: 400; Domain 2: 502
Map projection	Mercator
Reference coordinate	19°N, 133°E
Domain 2 starting grid number (southwest point)	East-West: 60; South-North: 175
Topography data	USGS
Atmospheric data	NCEP CFSv2 6-hourly Products
Time step	Domain 1: 30 s; Domain 2: 6 s
Pressure top	1000 Pa
Vertical layer	45
Nesting	One-way nesting (concurrent)
Microphysics	[2] Purdue Lin scheme (Chen & Sun, 2002)
Long-wave theory	[1] RRTM scheme (Mlawer et al., 1997)
Short-wave theory	[1] Dudhia scheme (Dudhia, 1989)
Surface layer option	[1] Revised MM5 scheme (Jimenez et al., 2012)
Land surface option	[4] Noah-MP land-surface model (Niu et al., 2011; Yang et al., 2011)
Planetary boundary condition	[1] YSU scheme (Hong et al., 2006)
Cumulus parameter	[2] Betts-Miller-Janjic scheme (Janjic, 1994)
FVCOM	
Simulation time	00:00 UTC August 7, 2015 - 00:00 UTC August 9, 2015
Latitude range	23.32° - 23.90°
Longitude range	119.57° - 120. 30°
Cells	50809
Nodes	26031
Mesh size	Nearly 100 - 5000 m
Vertical layer	11
Bathymetry data	Ocean Data Bank (200 m grid)
Coastline data	Modified based on SRTM3 (3 arc-second topography data)
Temperature & Salinity Boundary conditions	Blumberg & Kantha implicit radiation condition (Blumberg and Kantha, 1985)

3.2 Pseudo global warming using RCP scenarios

The study employed the pseudo global warming method (Sato et al. 2007) with global warming scenarios by applying various models included in the CMIP5. RCP4.5 and RCP8.5, listed in the Intergovernmental Panel on Climate Change 5th Assessment Report (IPCC AR5), were used to generate the future most likely and worst case global warming scenarios. Three parameters that are known to affect typhoon development, sea surface temperature (SST), atmospheric air temperature (AAT), and relative humidity (RH), were calculated, and the averaged values were taken as inputs into the simulation conditions (Nakamura et al. 2020). These three parameters were calculated by using five variables that are provided as outputs by the CMIP5 models: Sea Surface Temperature (sst, K), Air Temperature (ta, K), Near-Surface Air Temperature (tas, K), Relative Humidity (hur, %), and Near-Surface Relative Humidity (hurs, %). Simulations were performed for two different time horizons, 2041-2060 and 2081-2100, with the present baseline climate being considered to be that in the period 2006-2015. The detailed methodology of building pseudo global warming fields follows Nakamura et al. (2020).

To identify the sensitivity of the impact of each of these parameters (SST, AAT, and RH), simulations modifying only one single parameter and different combinations of two of the three parameters were also conducted. To reduce the potential bias caused by using a single global climate model (GCM), this study made use of an ensemble of 14 GCMs by following the criteria outlined in Mäll et al. (2020), see also supplementary information. The sea level rise (SLR) scenarios were also tested to see how global SLR would affect future storm surges in Taiwan. These simulations were conducted with the assumption that the future shape of the coastline would be the same as at present (i.e. essentially meaning that this will be fixed in place through the construction and/or reinforcement of coastal structures), and the SLR values (1.1m, 2.2m, and 2.92m) were directly added to the bathymetry data mesh generated by the surface-water modelling system (SMS; i.e. thus assuming no morphological changes).

4   Results

4.1 Simulation of Typhoon Soudelor under present day conditions

According to the typhoon database provided by Central Weather Bureau (CWB) in Taiwan, Typhoon Soudelor was first observed at 13.5°N, 161.0°E at 00:00 UTC on July 30th, 2015. The typhoon rapidly developed in intensity and reached its minimum centre pressure on August 4th, 2015. It then gradually decreased in intensity and hit Taiwan with a minimum sea-level pressure (MSLP) of 930 hPa and a maximum wind speed of 48 m/s (10-minute averaged). The simulation of Typhoon Soudelor was started on August 5th, 2015, which was three days before the typhoon reached the study area. Figure 4 shows that the simulated track remained north of the observed track before the typhoon made landfall in Taiwan. Figure 5 indicates that the minimum sea-level pressure is 3 hPa lower, and the maximum wind speed is 9 m/s higher than the observed values. This essentially means that the simulated typhoon is slightly stronger than the historical event.
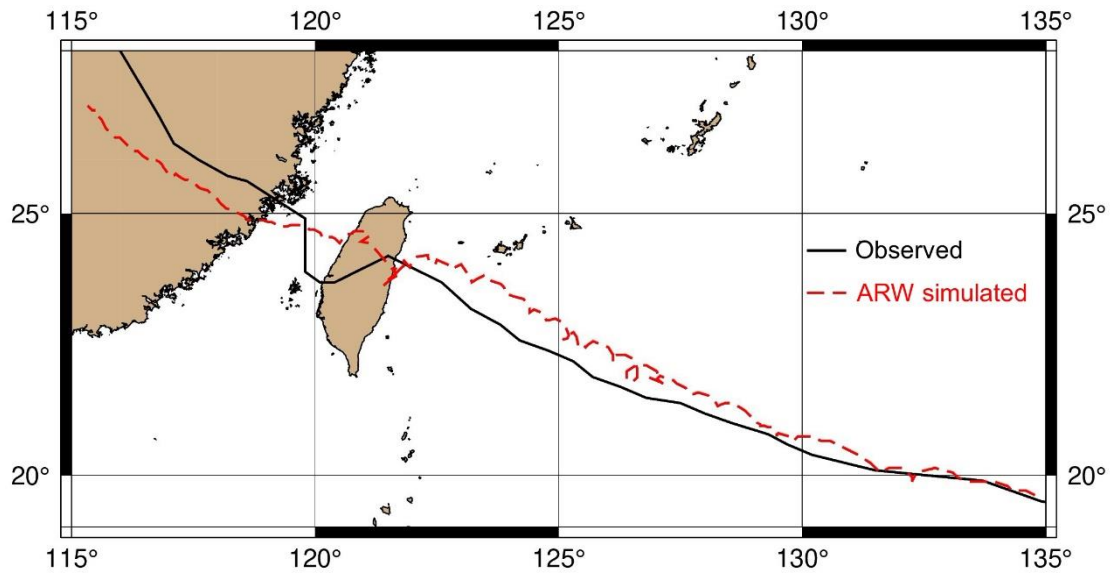
Figure 4: Observed historical typhoon track (CWB) and simulated typhoon track based on minimum sea level pressure (MSLP) in ARW results
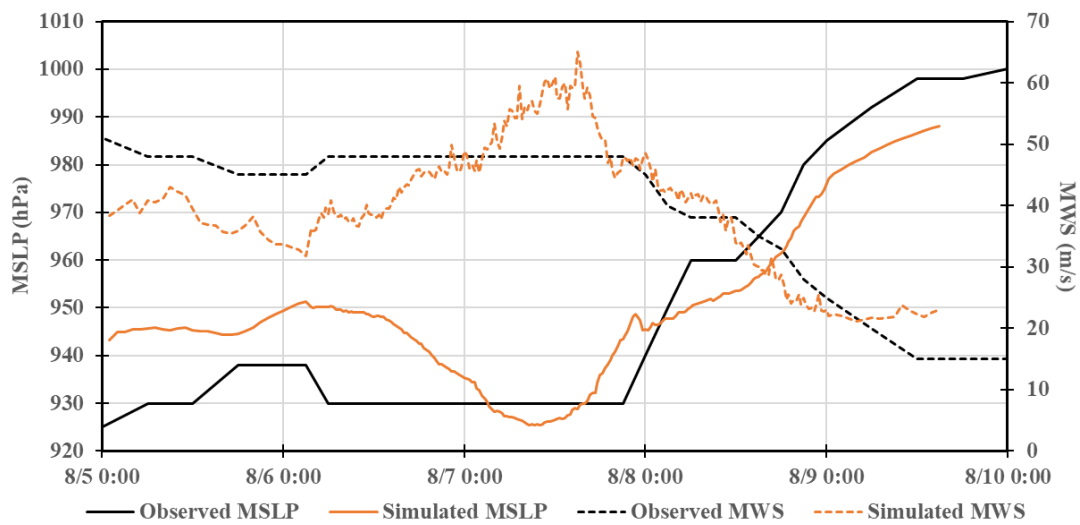

Figure 5: Comparison between observed minimum sea level pressure (MSLP) and maximum wind speed (MWS) from CWB and values simulated by ARW.

Figure 6 shows the sea level changes from 00:00 UTC August 7, 2015 to 00:00 UTC August 9, 2015 at Dongshi, Chiayi (see Figure 1b for the location of this tidal recording station). This station at Chiayi was chosen since the tidal station in Yunlin failed to record the change in sea level during the passage of Typhoon Soudelor. The estimated storm surge was calculated from data from CWB. Additionally, the difference between the tidal curve and the observed sea level (as shown in Figure 6) was measured manually (The maximum storm surge height (1.14 m) from Figure 6 is shown as a straight line in Figure 7).
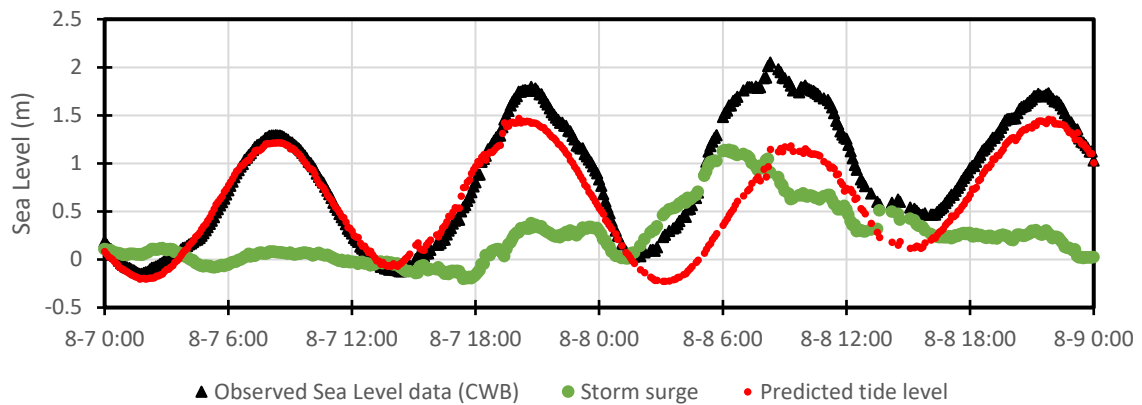
Figure 6: Observed sea level and storm surge at Dongshi Tidal station. Observed data were provided by CWB and storm surge data were calculated from the difference between observed sea level and predicted tidal changes (also from CWB).

The sea level changes shown in Figure 7 were calculated under present day atmospheric conditions, with the maximum simulated storm surge being slightly higher than the observed value (0.3 m higher; +26.3%). Figure 8 shows both the pressure and wind speed measured and simulated at the automatic meteorological observation station closest to Chiayi tidal station. The figure explains the possible reasons for the differences, as the simulated typhoon by WRF is stronger, thus leading to higher surge values at the Chiayi tidal station. While the simulation results were higher and the track followed slightly more northerly route, the model was still able to capture the two surge peaks. However, the first peak is slightly overestimated compared to the second peak (likely due to previously mentioned reasons).
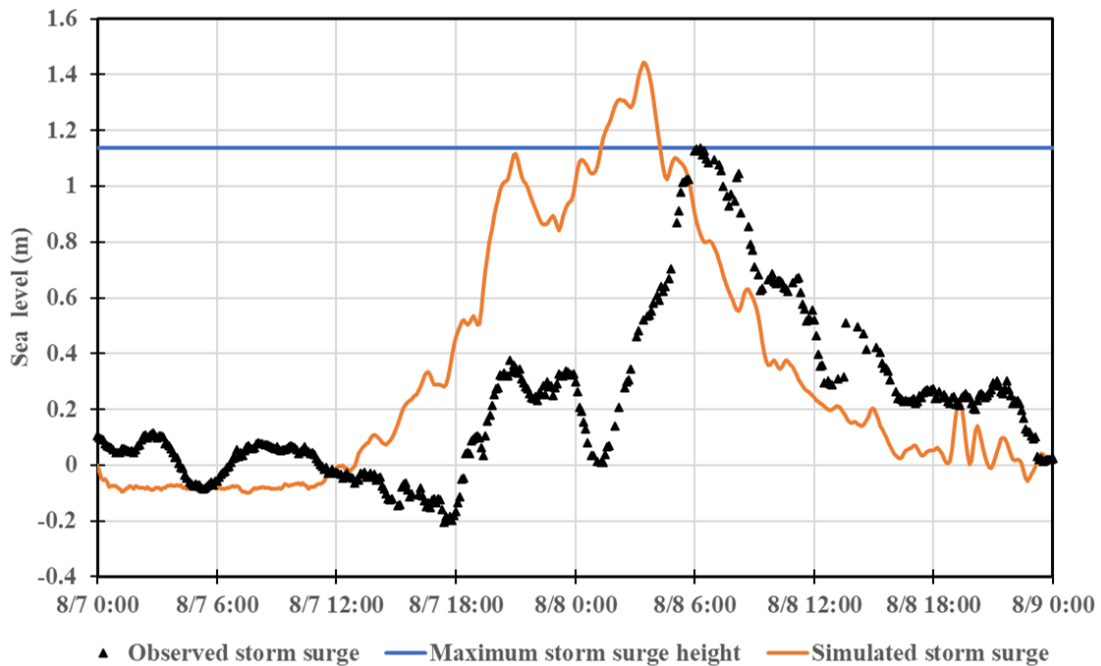

Figure 7: Storm surge simulated by FVCOM at Dongshi tidal station, Chiayi. The maximum simulated storm surge height was 1.44m
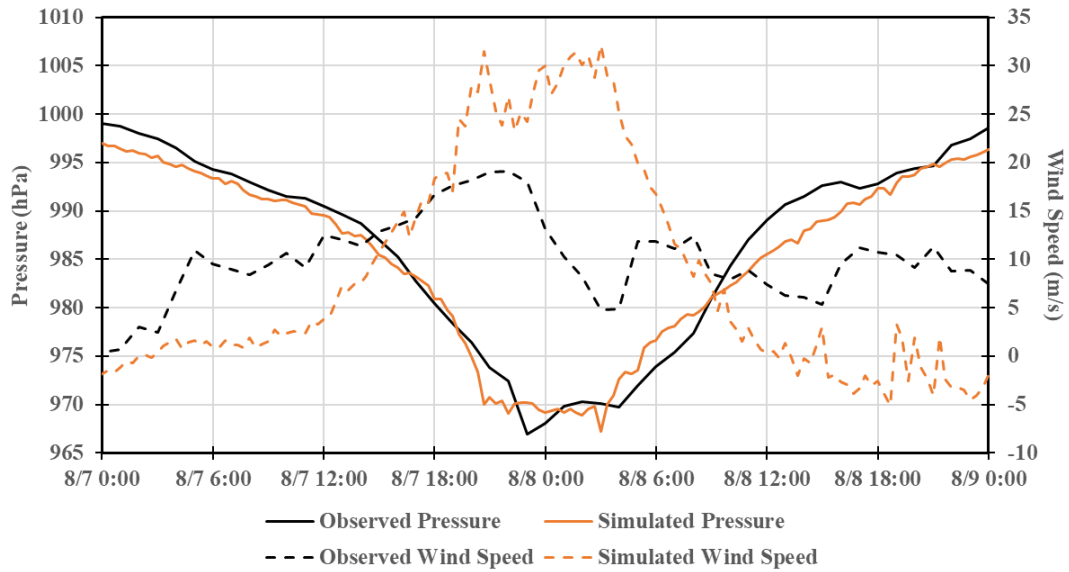
Figure 8: Simulated and observed (CWB) pressure and wind speed in Dongshi, Chiayi.

4.2 WRF results under RCP scenarios on CMIP5

For the future global warming scenario simulations, RCP4.5 and RCP8.5 were used to compare a stable and high greenhouse gas emissions scenario, respectively (see Figure A1 to A3 in Supplementary information). Many previous studies (e.g., Emanuel 1987; Knutson et al. 2010; Nakamura et al. 2016) indicate that sea surface temperatures (SST) is often the main factor increasing typhoon intensity, and to verify this in the present research a comparison among different combinations of the three parameters that were changed (SST, AAT, and RH) were conducted with ARW. These results are presented in Figure 9. The values of minimum sea-level pressure and maximum wind speed are listed in Table 2, which verified that SST has the biggest impact on the typhoon intensification. The addition of future climate atmospheric air temperature (AAT) fields also decreased the intensity of Typhoon Soudelor (relative to the present case), agreeing with the conclusion of Nakamura et al. (2016; 2020), likely due to a combination of reduced latent and sensible heat exchanges on air-sea surface (Emanuel et al. 1987) and decreased convective circulation (Wang et al. 2014). However, the change in relative humidity (RH) increased the maximum wind speed of the typhoon while keeping minimum sea-level pressure at similar values, which was different from the conclusion of Nakamura et al. (2016), who found that RH either has no impact on Typhoon Haiyan or slightly decreases its intensity. Table 3 shows the comparisons between this study and the simulation results from Nakamura et al. (2016). Some factors that might cause the differences, as shown in Table 3, include the different studied typhoon case, underestimation of simulated results discussed in Nakamura et al. (2016), the different simulated time horizons, and the method of calculating maximum wind speed. Nakamura et al. (2016) studied Typhoon Haiyan, which was a much stronger storm than Soudelor. Also, the simulations on Typhoon Haiyan was targeting the 2091~2100 time horizon, which was different from the results shown in the table (targeting 2081~2100) and used a single GCM model (MIROC5) instead of a multi-model ensemble. Furthermore, Nakamura et al. (2016) applied the empirical relationship by Atkinson and Holliday (1977) to calculate the maximum wind speed from minimum sea-level pressure, whereas the maximum wind speed in this paper were obtained directly from WRF outputs.

Table 2: Comparisons of minimum sea-level pressure (MSLP) and maximum wind speed (MWS) under 2081~2100 scenario and present conditions (red indicates stronger typhoons, blue indicates weaker typhoons).

	SST	SST,AAT	SST,AAT,RH	AAT	RH	SST,RH	Present
MSLP (hPa)							
RCP4.5	911.64	922.87	919.06	933.70	921.11	915.64	927.44
RCP8.5	904.69	919.62	919.53	948.47	926.71	898.84	927.44
MWS (m/s)							
RCP4.5	67.46	56.44	65.58	50.00	62.90	66.56	57.40
RCP8.5	68.44	61.10	68.50	44.27	57.81	76.27	57.40

Table 3: Comparisons of differences between simulated minimum sea-level pressure (MSLP) and maximum wind speed (MWS) under future scenarios and present day conditions (red indicates stronger typhoons, blue indicates weaker typhoons). (The average values were calculated for the four different scenarios for Nakamura et al. (2016) cases).

		MSLP (hPa)			MWS (m/s)		
		SST	SST,AAT	SST,AAT,RH	SST	SST,AAT	SST,AAT,RH
RCP4.5	Current study	-15.80	-4.57	-8.37	+10.06	-0.96	+8.18
	Nakamura et al. (2016)	-14.00	-9.00	-1.00	+4.30	+2.60	-1.40
RCP8.5	Current study	-22.75	-7.82	-7.90	+11.04	+3.70	+11.11
	Nakamura et al. (2016)	-22.00	-13.00	-4.00	+7.80	+4.10	+0.10
Average of all RCP scenarios	Current study	-19.27	-6.19	-8.14	+10.55	+1.37	+9.65
	Nakamura et al. (2016)	-13.50	-9.25	-2.25	+4.20	+2.48	-0.65
Average difference of all RCP scenarios compared to simulated present day condition results in percentage (%)	Current study	-2.08	-0.67	-0.88	+18.39	+2.39	+16.80
	Nakamura et al. (2016)	-1.47	-1.01	-0.25	+6.36	+3.75	-0.98

Overall, while the two studies present several differences regarding the simulation conditions, they still showed similar trend in positive/negative impact on typhoon development when modifying the three parameters. Figure 10 shows the simulation of the typhoon track for the various combinations of changes in these three parameters. Although SST and AAT had a large impact on the intensity of typhoons, they had very little effect on typhoon tracks. On the other hand, changes in RH were the main factor making the simulated typhoon tracks deviate from the historical path. Particularly, for the RCP8.5 2081~2100 time horizon, the simulated typhoon drastically turns south as it approaches Taiwan. Several authors that have studied typhoons passing through mountain areas, including the Central Mountain Range in Taiwan, indicate that these weather systems can be deflected due to the channeling effect, vortex stretching, and asymmetric diabatic heating when their structures are blocked by mountains (Hsu et al., 2018, Chen et al., 2002, Chang et al., 2017). Interestingly, these results (as seen in Figures 9 and 10) indicate that while typhoons go through different levels of intensification over the open ocean (e.g. large differences in maximum wind speed and minimum sea-level pressure between SST and AAT only cases), they also tend to streamline once make landfall and start crossing the Central Mountain Range. This tendency is especially evident for the maximum wind speed changes under both RCP4.5 and RCP8.5 scenarios (Figures 9b and 9d after 8/7 12:00 UTC). The wind fields simulated for the RCP8.5 2081~2100 time horizon are shown in the Supplementary Information.

The storm surge simulations under future scenarios (SST, AAT, RH) conducted with FVCOM also covered two RCP scenarios for two different time horizons. These simulated water level results are shown in Figure 11. For the case of RCP4.5, the maximum storm surge heights at Chiayi tidal station were 1.41 m and 1.61 m for 2041~2060 and 2081~2100, respectively. For the same time horizons under RCP8.5, the surge values became 1.51 m and 1.52 m, respectively. Comparing to the 1.43 m under present day conditions, both RCP scenarios for the 2041~2060 horizon showed differences of less than 0.1 m, indicating that only by the end of the century significant increases in storm surge height in the study area will likely take place. However, it is important to note that the time history curve for the case of RCP8.5 2081~2100 time horizon is very different from that of the other scenario and present day conditions. The sudden initial drop in sea level in this scenario is due to the simulated typhoon track deviating southwards (compared to the other simulation cases), similar to the cause of the 0.3 m storm surge height difference between the observed historical data and the simulated present case conditions, as discussed earlier. However, the deviation in this case was much more significant, making the wind field for this scenario markedly different from the other three simulations (see Figure A5 in Supplementary information). As for the timing of the arrival of storm surges, the simulation cases targeting the 2081~2100 time horizon both generate storm surges earlier, which was caused by the faster typhoon moving speed. Table 4 shows the time of typhoon centre entering the storm surge simulation domain.
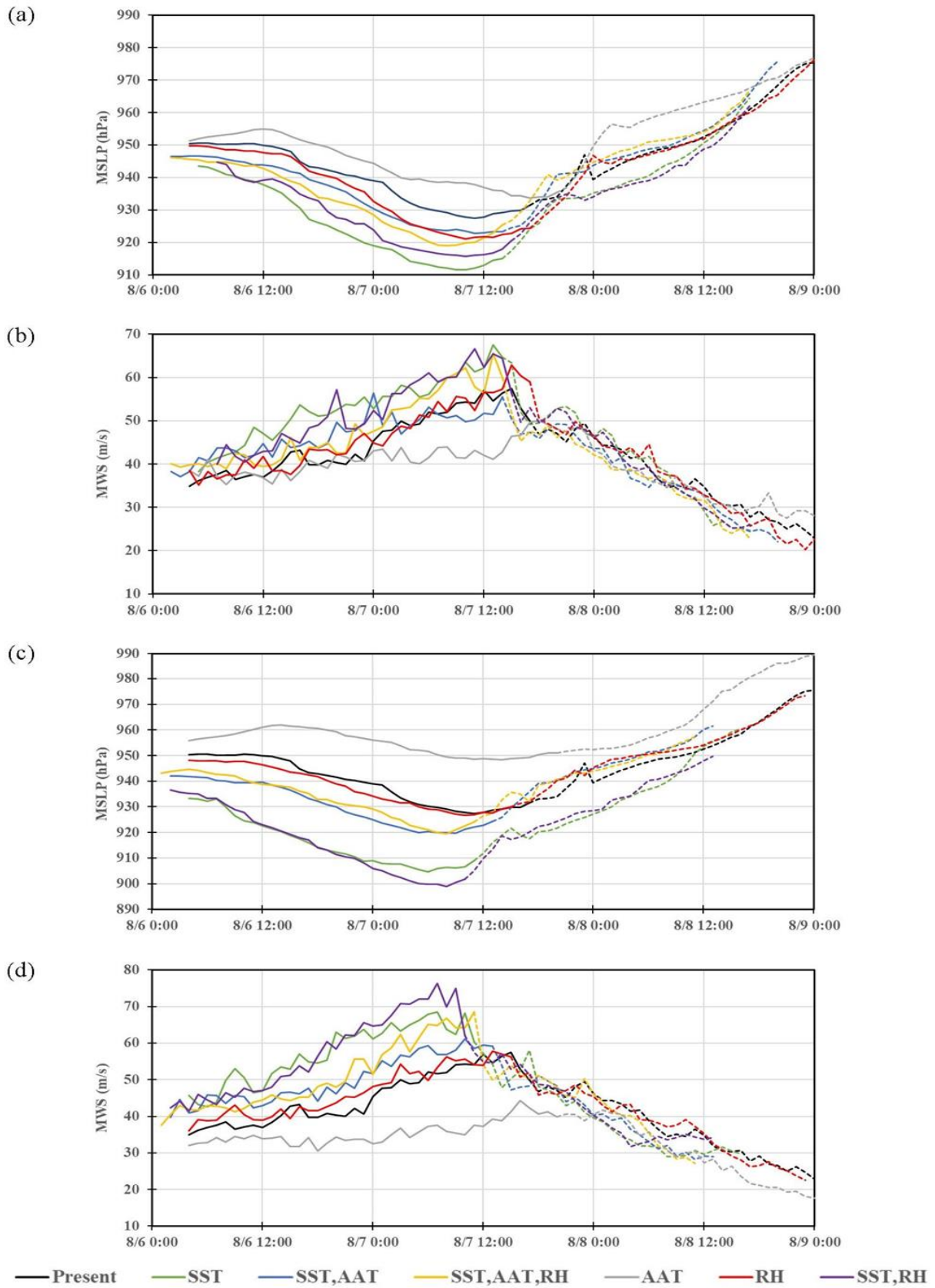
(a)

(b)

(c)

(d)

Figure 9: Minimum sea-level pressure (MSLP) and maximum wind speed (MWS) with modifications on SST, AAT, and RH under RCP4.5 (a)(b) and RCP8.5 (c)(d) for 2081~2100 (The curves are shown as dashes after the typhoon centre crosses the 122.5°E longitude line).
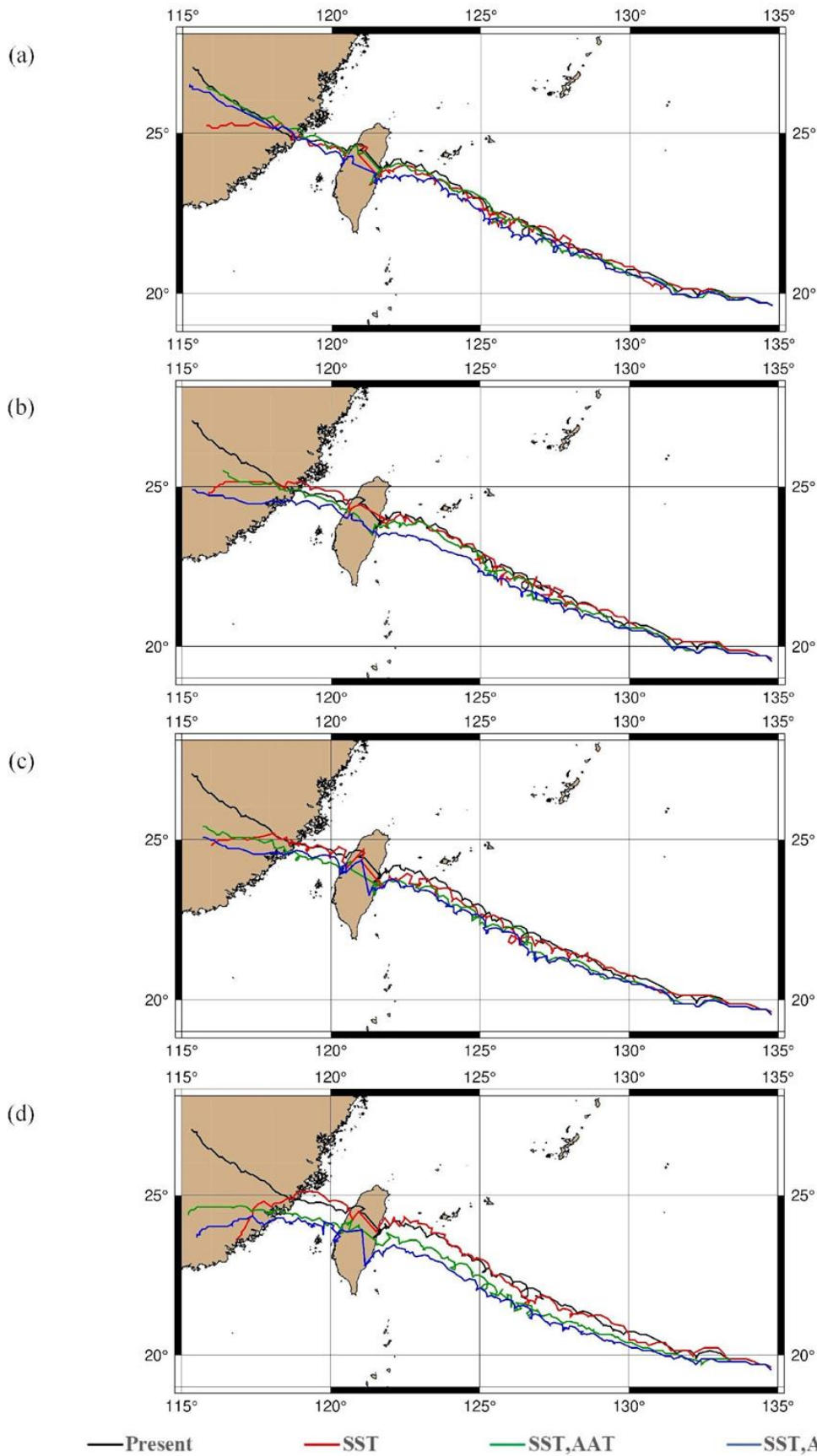
Figure 10: Typhoon tracks with CMIP5 modification (a) RCP4.5 2041~2060 (b) RCP4.5 2081~2100 (c) RCP8.5 2041~2060 (d) RCP8.5 2081~2100.
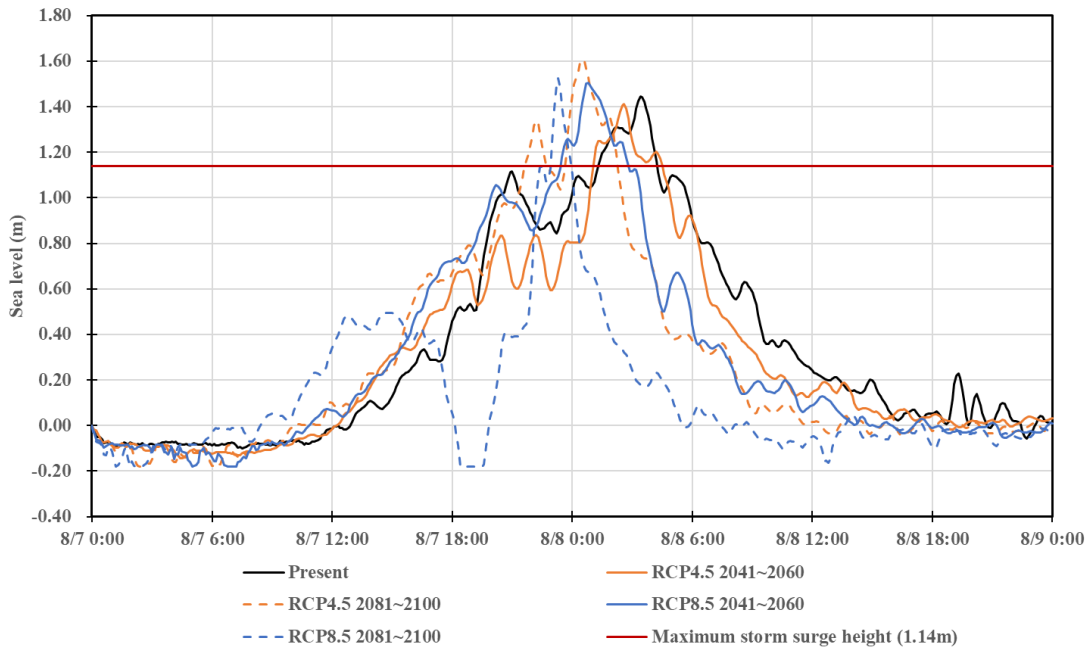
Figure 11: FVCOM storm surge simulation under different RCP scenarios. The RCP scenarios include all 3 parameters (SST, AAT and RH).

Table 4: Summary of typhoon centre entering the storm surge simulation domain for different scenarios

Present	RCP4.5 2041~2060	RCP4.5 2081~2100	RCP8.5 2041~2060	RCP8.5 2081~2100
8/8 02:40	8/8 00:40	8/7 23:40	8/7 23:20	8/7 19:00

4.3   FVCOM results considering SLR under RCP scenarios

In order to include the effect of sea level rise (SLR) into the FVCOM simulations, the average water depth throughout the computational domain was raised according to a number of scenarios, always assuming that the location of the coastline remains constant (which in turn assumes that coastal structures will be built and/or raised to compensate for SLR). The first scenario considered a SLR 1.1m, which is the maximum value for the global average SLR by 2100 under RCP8.5 suggested in a Special Report of the Intergovernmental Panel on Climate Change (SROCC; IPCC, 2019). The second scenario considered a SLR of 2.2m, as several authors have indicated that the rate of SLR around Taiwan for the past decades was much faster than the global average (Huang et al., 2010, Tseng et al., 2010, Kuo et al., 2015). Kuo et al. (2014) indicate that the SLR rate for Taiwan could even be twice that of the global average (hence the value of 2.2 m for this scenario). The third scenario considered a SLR of 2.92 m, following the high end projections by Le Bars et al. (2017). The FVCOM simulations were conducted using the modified bathymetry data according to these SLR scenarios and the previously simulated typhoons using the modified SST, AAT and RH data under RCP8.5 2081~2100 time horizon.

4.3.1 Dongshi tidal station

The simulated time history of the storm surges at Dongshi tidal station is shown in Figure 12, and the maximum values of these storm surge heights are provided in Table 5. The contribution of the storm surge height alone decreases as the SLR value increases, which was expected due to the increase of water depth, given that the study area has a shallow average water depth. This is easily understood by the simplified force balance between a shoreward directed wind stress τ_w and the pressure gradient resulting by a coastal storm surge of height y generated by a wind blowing over a continental shelf or fetch of length L, as shown by eq (1):

$$y = \frac{\tau_w L}{\rho g h} \tag{8}$$

where h is the water depth, g is the acceleration due to gravity and ρ is the water density.

Table 5: Storm surge height for different SLR scenarios at Dongshi tidal station, Chiayi. The RCP scenarios include all 3 parameters (SST, AAT and RH)

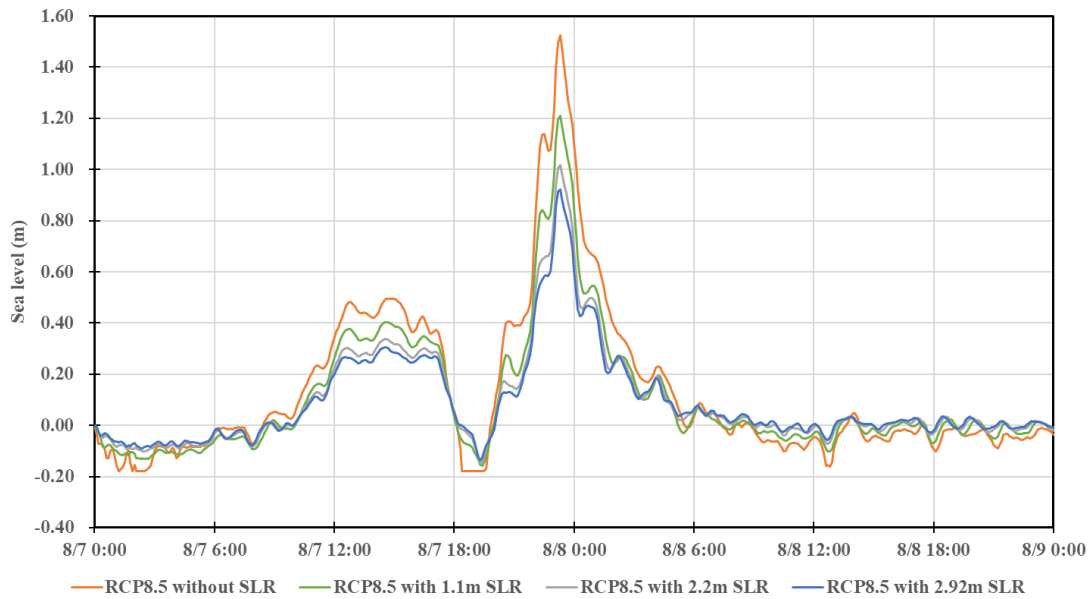|	No SLR	1.1m SLR	2.2m SLR	2.92m SLR
Storm surge height (m)	1.52	1.21	1.02	0.92
Decrease of storm surge height compared to original value (1.52m) (%)	-	20.75	33.23	39.63
Total sea level increase (Storm surge + SLR) (m)	1.52	2.31	3.22	3.84

Figure 12: Sea level at Dongshi tidal station under RCP8.5 for different SLR simulations. The RCP scenarios include all 3 parameters considered in this study(SST, AAT and RH)

Equation (8) shows that a larger mean water depth h results in a lower storm surge height y for a given storm strength (wind stress) or storm size (fetch length). SLR has the effect of increasing this mean water depth h, thus reducing the height of the storm surge y. However, the actual coastal water level during a storm is not just storm surge, but the storm surge plus the ambient water level ($h+y$). Therefore, even though SLR causes a reduction in storm surge, the actual water level ($h+y$) is still larger than the no-SLR case, due to the increased mean water level h.

The decreases in the simulated maximum value of the storm surge for RCP8.5 scenarios (no SLR vs. SLR) were 0.31 m, 0.50 m, and 0.60 m for the1.1 m, 2.2 m and 2.92 m SLR scenarios, respectively. This means that while the storm surge height itself will decrease, the compounded effect (the total water level increase due to both storm surge and SLR) will still be considerable (reaching 3.84 m for the 2.92 m SLR scenario).

4.3.2 Bozilao tidal station

The previous comparisons were all performed at Dongshi tidal station in Chiayi, the county next to Yunlin, due to the lack of observed data in Yunlin for the case of the Typhoon Soudelor. To have a better understanding of the future storm surges at Yunlin, the storm surges at Boziliao tidal station at Yunlin (as shown in Figure 1b) are shown in Figure 13 and Table 6 for each of the scenarios outlined earlier. Although the two tidal stations (i.e. Dongshi and Boziliao) show similar simulated storm surge under present day conditions, all of the other potential future cases indicate that the surge at Yunlin would probably decrease.
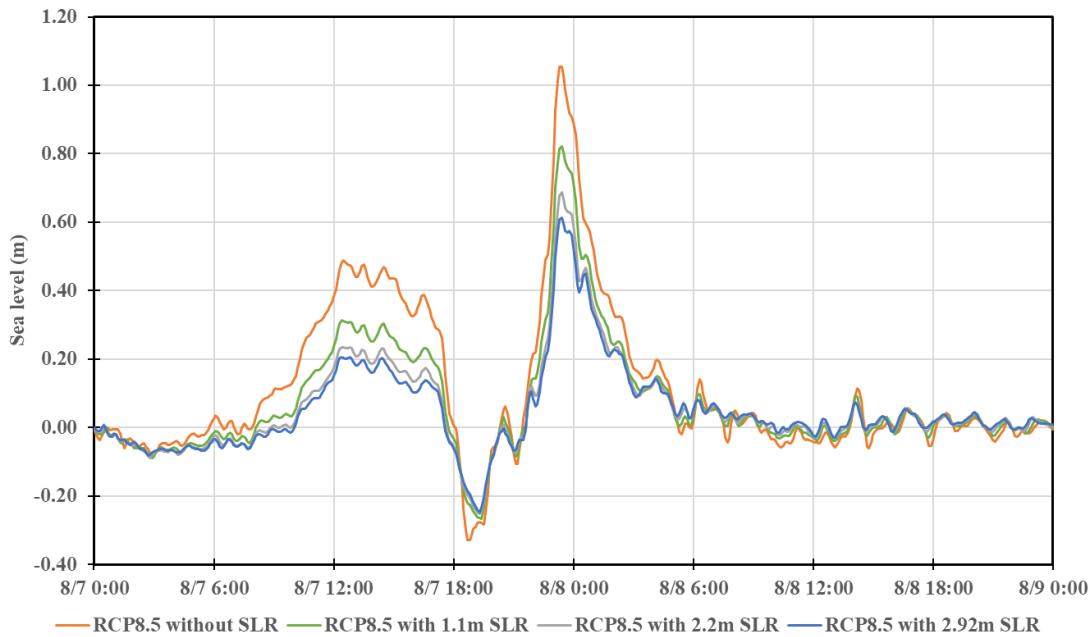
Figure 13: Sea level at Boziliao tidal station under RCP8.5 with different SLR simulations. The RCP scenarios include all 3 parameters (SST, AAT and RH).

Table 6: Storm surge height and the decrease of storm surge (in percentage) at Boziliao under different SLR scenarios. The RCP scenarios include all 3 parameters (SST, AAT and RH).

	No SLR	1.1m SLR	2.2m SLR	2.92m SLR
Storm surge height (m)	1.05	0.82	0.69	0.61
Decrease of storm surge height compared to original value (1.05m) (%)	-	22.06	34.87	41.79
Total sea level increase (Storm surge + SLR) (m)	1.05	1.92	2.89	3.53

5   Discussion

The WRF simulation results after performing the CMIP5 modification on SST, AAT, and RH not only change the typhoon intensity but also cause a deviation in the typhoon track, especially when changing the RH parameter. This in turn greatly influenced the simulated storm surges for the various scenarios, especially when the typhoon tracks deviated further toward the south and passed through the study area, showing the importance of accurately simulating the typhoon track. One common method to increase the accuracy of typhoons is tropical cyclone initialization. The default Tropical Cyclone Bogus package in WRF is a simple way to perform this tropical cyclone initialization and was tested on Typhoon Morakot (Chang et al., 2019) and Typhoon Haiyan (Nakamura et al., 2016), showing a general increase in accuracy. However, the tests on Typhoon Soudelor using a similar method did not work well in the present case. Chang et al. (2017) tested the Nguyen and Chen (2011) tropical cyclone initialization method before running WRF and were able to obtain more accurate typhoon structures. The TWRF system used by the Central Weather Bureau (CWB) in Taiwan also applies another tropical cyclone initialization scheme before the start of the simulations (Hsiao et al., 2010), showing that a proper initialization could be as important as choosing suitable physics settings for each typhoon case or study area.

The pseudo-global warming method used in this study further reaffirmed findings from similar studies that investigate the typhoon evolution under modified sea surface temperatures (SST), atmospheric air temperatures (AAT) and relative humidity (RH) future conditions (e.g. Nakamura et al. 2016). The findings indicate that typhoons are likely to be intensified when considering only increased SST, though taking into account AAT fields dampen such increases in intensity. It was further found that this intensification (mainly maximum wind speed) tended to streamline once landfall was made in the eastern coast of Taiwan, and the typhoons started to propagate over the Central Mountain Range. It is therefore possible that, even if stronger typhoons approach and cross the Central Mountain Range, the mountain range can significantly dampen such storms (e.g. maximum wind speed, as see in Figure 9b and 9d). This means that while

more intense future typhoons can approach the eastern coast of Taiwan, the western coast (and other westward regions along the track) might not feel the full force of such weather extremes due to the shielding effect caused by the Central Mountain Range. However, these findings would benefit from future research, considering more typhoon cases studies and analysis.

The results of the simulations under future SLR scenarios indicate that raising water levels will dampen the height of the storm surges in the area. While this may appear counter-intuitive, the wind-driven storm surge component is inversely proportional to water depth, as the force balance that predicts the free surface slope is equal to the wind stress divided by the water depth (Equation 8). SLR will result in deeper water, and assuming no morphological changes in the study area, this will result in a smaller free surface gradient (and therefore less overall surge).

From the previous discussion and the future SLR scenarios simulations, it is clear that small changes in water depth can greatly affect the simulated storm surge in the study area. In this sense, it is also worth noting that the water depth in the area is also affected by tidal changes, and that there are issues related to the bathymetry data used. In that sense, the authors note that the bathymetry data provided by the Ocean Data Bank (ODB) does not match the coastline data in the Shuttle Radar Topography Mission with 3 arc-sec resolution (SRTM3), and that there are also differences with the widely utilized bathymetry data source *The General Bathymetric Chart of the Oceans (GEBCO)*. One of the most obvious examples would be the location of Waisanding Sandbar, the largest barrier island along the coastline in Taiwan. The sandbar is around 10 km away from the coastline of Chiayi and Yunlin County, with a land area of hundreds of hectares during high tides and thousands of hectares during low tides protecting it from the direct action of waves (Peng et al., 2019). However, the sandbar is not shown in either of the bathymetry data sources and could potentially be one of the reasons why the simulated storm surges in FVCOM under present day conditions was slightly overestimated. Other land that can be seen on satellite images but is not captured in the data includes the location of the sixth naphtha cracker in Yunlin, several land reclamation projects, and the existence of coastal wetlands. All these factors make the accurate simulation of storm surges in the study area challenging, especially for future scenarios where coastline changes that were not considered in this study might also take place. According to Lin et al. (2003), Waisanding Sandbar has become smaller due to river rehabilitation and construction along the coastline since 1973, blocking the sediments transport from Zhoushui River, the main source of sediments for the sandbar. This would not only damage the local environment, but at the same time further increase the risk of direct damage to coastal protection structures from waves.

Furthermore, the simulations performed in this study did not include the influence of land subsidence. This has severely affected the study area for several decades, with Yunlin and Chiayi County continuing to subside at an average rate of 2~3 cm per year (with even faster rates recorded at inland areas; Information of Land Subsidence Prevention in Taiwan, 2020). This represents a particular threat to existing coastal structures (Ke et al., 2021) and, compounded with the effects of SLR, land subsidence and stronger typhoons, will likely result in them facing even higher water levels in decades to come. It is thus imperative that all such factors are taken into account when considering the maintenance and upgrade of such structures, which are highly likely to become more expensive as the 21st century progresses.

Finally, it is worth noting that it is expected that climate change could change other characteristics of tropical cyclones around the planet, including their translate speed, with some evidence existing that this could already be happening (Inagaki et al., 2021). This could have a large effect on their wind field and, consequently, on the waves generated by such a typhoon, in turn impacting the size of the storm surge. The waves generated by large typhoons could increase in size if they accelerate just before landfall (Inagaki et al., 2021), and this could affect the stability of coastal structures, which would have to withstand higher waves and storm surges.

6   Conclusions

The present study simulated the potential consequences that the intensification of typhoons due to climate change and SLR could have on coastal defences in western Taiwan, using WRF-ARW to simulate typhoons and FVCOM to estimate the storm surges generated by them. WRF-ARW was verified by simulating the historical typhoon Soudelor in 2015, with the results showing good agreement with the observed data provided by Central Weather Bureau (CWB) of Taiwan (with a small difference in typhoon track due to the influence of the Central Mountain Range of the country). The difference between observed and simulated storm surge heights was around 0.3 m, with the error being partly explained by the

inaccuracy of the coastline and bathymetry data (which did not show several reclaimed lands, wetlands, and sandbars in the simulation domain).

Future typhoon scenarios were modelled by modifying three parameters, SST, AAT, and RH in 14 GCMs from CMIP5 provided by several institutes. The results showed that the typhoons increased in strength when the SST rose, though increasing AAT had a negative effect on typhoon developments. Increases in RH slightly increased the intensity of the typhoon, though they led to larger deviations in the typhoon track from that of the historical storm. Furthermore, the large deviation in the RCP8.5 2081~2100 resulted in significant changes in wind fields and the time history of the storm surge. By including different SLR scenarios into the storm surge simulations, the estimated maximum water height decreased 20% to 40%. Nevertheless, the combined effect of SLR and storm surge could result in total water levels reaching +3.84 m for the worst scenario case.

While the results in this study suggest more intense future typhoons (with the exception of AAT only case), they also become streamlined once they start to cross the Central Mountain Range. These findings indicate that it is possible for stronger future typhoons to be considerably dampened during their passage over the Central Mountain Range, which provides a shielding effect for the west coast. For future research the authors recommend to further investigate the impact of the Central Mountain Range on future typhoons that are intensified by climate change

This study concludes that the maximum water levels due to storm surges, land subsidence and SLR in Yunlin and Chiayi County could slightly increase in the future. However, further study on the changes of wind wave patterns on storm surge levels is needed due to the significant increase in wind speed, and the effect of tidal changes should also be considered (given that the present study showed that the storm surge levels in this area are heavily influenced by changes in the shallow water depth). As a result, it is clear that much more research is needed to ensure the coastal defences in the area can be adequately maintained and upgraded in the future, and the risks that climate change poses to the long-term sustainability of human settlements.

Acknowledgements

Author contributions (CRediT)

Yuchia Chang[1]: Research Formulation, Data Gathering, Computer Simulations, Writing – original draft, Martin Mäll[2], Computer Simulations, Methodological Framework, Computer Modelling Support, Writing – review & editing, Ryota Nakamura [3], Methodological Framework, Computer Modelling Support, Tomoyuki Takabatake [4], Writing – review & editing, Jeremy Bricker [5], Writing – review & editing, Miguel Esteban [6], Supervision, Writing – review & editing, Tomoya Shibayama [7], Supervision, Writing – review & editing.

Notation and abbreviations

Name	Abbreviation
WRF-ARW	The Advanced Research Weather Research and Forecasting Model
FVCOM	The Unstructured Finite Volume Community Ocean Model
CWB	Central Weather Bureau
SLR	Sea level rise
TWRF	Typhoon Weather Research and Forecasting Model

SWAN	The Simulating Waves Nearshore
ADCIRC	The Advanced CIRCulation
GCMs	General circulation models
SST	Sea surface temperature
AAT	Atmospheric air temperature
RH	Relative humidity
CMIP5	Coupled Model Intercomparison Project Phase 5
NCDR	National Science and Technology Centre for Disaster Reduction
WPS	WRF Preprocessing System
NCAR	National Centre for Atmospheric Research
ODB	Ocean Data Bank
SRTM3	Shuttle Radar Topography Mission 3 arc-second
SMS	Surface-water Modelling System
WSF	WRF Software Framework
NCEP	National Centres for Environmental Prediction
CFSv2	Climate Forecast System Version 2
MSLP	Minimum sea-level pressure
MWS	Maximum wind speed
FEM	Finite-element method
RCP	Representative concentration pathways
IPCC AR5	The Intergovernmental Panel on Climate Change 5th Assessment Report
sst	Sea surface temperature (CMIP5 models)
ta	Air temperature (CMIP5 models)
tas	Near-surface air temperature (CMIP5 models)
hur	Relative humidity (CMIP5 models)
hurs	Near-surface relative humidity (CMIP5 models)
GCM	Global climate model
SROCC	Special Report of the Intergovernmental Panel on Climate Change
GEBCO	The General Bathymetric Chart of the Oceans
JST	Japan Science and Technology Agency

References

Atkinson, G. D., & Holliday, C. R. (1977). Tropical Cyclone Minimum Sea Level Pressure/Maximum Sustained Wind Relationship for the Western North Pacific, Monthly Weather Review, 105(4), 421-427. Retrieved Jul 17, 2021, from https://journals.ametsoc.org/view/journals/mwre/105/4/1520-0493_1977_105_0421_tcmslp_2_0_co_2.xml

Blumberg, A. F. and L. H. Kantha, 1985. Open boundary condition for circulation models. J. Hydraul. Eng., 111, 237-255.

Central Emergency Operation Center. (2015). 蘇迪勒颱風災害應變處置報告第 9 報 (The 9th Emergency Response Report for Typhoon Soudelor). [in Mandarin]

Central Weather Bureau Typhoon Database. https://rdc28.cwb.gov.tw/TDB/. Accessed 25 July, 2021.

Chang, C. H., Wang, Y. T., Fu, H. S., Lin, Y. C., Chang, C. H., Liu, C. H., Lu, C. Y., Wu, C. J., & Su, Y. F. (2015). 2015 年蘇迪勒颱風災害調查彙整報告 (Disaster report on Typhoon Soudelor in 2015). National Science and Technology Center for Disaster Reduction. [in Mandarin]

Chang, C. W. and Chien, F. C. (2017). Numerical Simulation and Study of Typhoon Soudelor (2015). [Master's Thesis, Department of Earth Sciences, National Taiwan Normal University]. http://rportal.lib.ntnu.edu.tw:80/handle/20.500.12235/101189. [in Mandarin]

Chang, G. T., Chiu, C. M., Chang, G. C., Doong, D. J., & Chen, H. L. (2004). Regression Analysis on the Typhoon Surge in Taiwan. http://www.tsoe.org.tw/downloads/thesis/2004C8.pdf. [in Mandarin]

Chang, Y. C. (2019). Estimating Influence of Sea Level Rise and Climate Change on Coastal Defences in Western Taiwan using WRF-FVCOM Model. Master's Thesis, Department of Civil and Environmental Engineering, School of Creative Science and Engineering, Waseda University.

Chang, Y. H. (2008). Storm Surge Analysis Considering Atmospheric Pressure Variation. Master's Thesis, Institute of Civil Engineering National Chiao Tung University. https://ir.nctu.edu.tw/bitstream/11536/38698/1/654101.pdf. [in Mandarin]

Chen, S. H. and Sun, W. Y. (2002). A one-dimensional time dependent cloud model. J. Meteor. Soc. Japan., 80(1), 99–118. doi:10.2151/jmsj.80.99

Chen, S. Y. and Huang, C. Y. (2002). 地形對颱風路徑的影響之數值探討. A numerical study of the influence of topography on typhoon tracks. Master's Thesis, Department of Atmospheric Sciences, College of Earth Sciences, National Central University. https://hdl.handle.net/11296/ga5p23. [in Mandarin]

Chou, S. Y., Lin, P. L., & Chen, Y. N. (2017). 渦旋初始化方法對熱帶氣旋模擬之影響 — 蘇迪勒颱風(2015)個案. The influence of vortex initialization on tropical cyclones simulations – Typhoon Soudelor (2015) case study. Master's thesis, National Central University. http://pblap.atm.ncu.edu.tw/thesis/GT/GT201706084806/201706084806.pdf. [in Mandarin]

Directorate-General of Budget, Accounting and Statistics, Executive Yuan, R.O.C. (2020). National Statistics. http://statdb.dgbas.gov.tw/pxweb/Dialog/statfile9.asp. [in Mandarin]

Dudhia, J. (1989). Numerical study of convection observed during the Winter Monsoon Experiment using a mesoscale two–dimensional model. J. Atmos. Sci., 46, 3077–3107. doi:10.1175/1520-0469(1989)046<3077:NSOCOD>2.0.CO;2

Dobrynin M, Murawsky J, Yang S. (2012). Evolution of the global wind wave climate in CMIP5 experiments. Geophys. Res. Lett., vol. 39, L18606, doi:10.1029/2012GL052843

Emanuel, K. 1987. The Dependence of Hurricane Intensity on Climate. Nature 326: 483–485. doi:10.1038/326483a0.

Fakour, H., Lo, S.-L., Lin, T.-F. (2016). Impacts of Typhoon Soudelor (2015) on the water quality of Taipei, Taiwan. Scientific Reports (6), 25228.

Hill K. A. and Lackmann, G. M. (2009) Influence of Environmental Humidity on Tropical Cyclone Size, 137(10): 3294–3315. DOI: https://doi.org/10.1175/2009MWR2679.1

Honda, C. and Mitsuyasu, K. (1980). Laboratory study on wind effect to ocean surface. J Coast Eng JSCE 27:90–93

Hong, S. Y., Noh, Y., & Dudhia, J., (2006). A new vertical diffusion package with an explicit treatment of entrainment processes. Mon. Wea. Rev., 134, 2318–2341. doi:10.1175/MWR3199.1

Hsiao, L., Liou, C., Yeh, T., Guo, Y., Chen, D., Huang, K., Terng, C., & Chen, J. (2010). A Vortex Relocation Scheme for Tropical Cyclone Initialization in Advanced Research WRF, Monthly Weather Review, 138(8), 3298-3315. Retrieved Jul 6, 2021, https://journals.ametsoc.org/view/journals/mwre/138/8/2010mwr3275.1.xml.

Hsiao, L. F., Chen, D. S., Hong, J. S., Yeh, T. C., & Fong, C. T. (2020). Improvement of the Numerical Tropical Cyclone Prediction System at the Central Weather Bureau of Taiwan: TWRF (Typhoon WRF). Atmosphere 11, no. 6: 657. https://doi.org/10.3390/atmos11060657.

Hsu, L. H., Su, S. H., Fovell, R. G., & Kuo, H. C. (2018). On Typhoon Track Deflections near the East Coast of Taiwan. Monthly Weather Review, 146(5), 1495-1510. Retrieved Jun 19, 2021, from https://journals.ametsoc.org/view/journals/mwre/146/5/mwr-d-17-0208.1.xml. DOI: 10.1175/MWR-D-17-0208.1

Huang, C. C., Hsu, T. W., and Wu, L. C. (2010). 運用潮位與衛星資料推估海平面變遷量技術之研發(2/2), Water Resources Agency, MOEA. [in Mandarin]

Inagaki, N., Shibayama, T., Esteban, M. and Takabatake, T., Effect of Translate Speed of Typhoon on Wind Waves (2021) Natural Hazards, 105 (1), 841-858.

Information of Land Subsidence Prevention in Taiwan. (2020). Current situation of land subsidence in Yunlin. http://www.lsprc.ncku.edu.tw/zh-tw/trend.php?action=view&id=18. Accessed 25 July 2021 [in Mandarin]

IPCC, 2019: IPCC Special Report on the Ocean and Cryosphere in a Changing Climate [H.-O. P¨ortner, D.C. Roberts, V. Masson-Delmotte, P. Zhai, M. Tignor, E. Poloczanska, K. Mintenbeck, A. Alegrí a, M. Nicolai, A. Okem, J. Petzold, B. Rama, N. M. Weyer (eds.)]. In press.

Janjic, Z. I. (1994). The Step–Mountain Eta Coordinate Model: Further developments of the convection, viscous sublayer, and turbulence closure schemes. Mon. Wea. Rev., 122, 927–945. doi:10.1175/1520-0493(1994)122<0927:TSMECM>2.0.CO;2

Jee, J and Kim, S. (2017). Sensitivity Study on High-Resolution WRF Precipitation Forecast for a Heavy Rainfall Event. Atmosphere. 8. 96. 10.3390/atmos806006.

Jiménez, P. A., Dudhia, J., González-Rouco, J. F., Navarro, J., Montávez, J. P., & García-Bustamante, E. (2012). A Revised Scheme for the WRF Surface Layer Formulation, Monthly Weather Review, 140(3), 898-918. Retrieved Jul 16, 2021, from https://journals.ametsoc.org/view/journals/mwre/140/3/mwr-d-11-00056.1.xml

Kanada, S., Takemi, T., Kato, M., Yamasaki, S., Fudeyasu, H., Tsuboki, K., Arakawa, O., & Takayabu, I. (2017). A multimodel intercomparison of an intense typhoon in future, warmer climates by four 5-km-mesh models, Journal of Climate, 30(15), 6017-6036. doi:10.1175/JCLI-D-16-0715.1.

Ke, Q., Yin, J., Bricker, J. D., Savage, N., Buonomo, E., Ye, Q., Visser, P., Dong, G., Wang, S., Tian, Z., Sun, L., Tuomi, R., & Jonkman, S. N. (2021). An integrated framework of coastal flood modelling under the failures of sea dikes: a case study in Shanghai, Natural Hazards, 1-33.

Knutson, T. R., J. L. McBride, J. Chan, K. Emanuel, G. Holland, C. Landsea, I. Held, J. P. Kossin, A. K. Srivastava, and M. Sugi. 2010. Tropical Cyclones and Climate Change. Nature Geoscience 3: 157–163. doi:10.1038/ngeo779.

Knutson, T., Camargo, S. J., Chan, J. C. L., Emanuel, K., Ho, C-H., Kossin, J., Mohapatra, M., Satoh, M., Sugi, M., Walsh, K., Wu, L. (2020) Tropical cyclones and climate change assessment: Part II: Projected response to anthropogenic warming, Bulletin of the American Meteorological Society 101(3), E303-E322.

Kuo, C. Y., Lin, L. C., Lan, W. H., Chuang, W. C., & Li, C. Y. (2014). 臺灣四周海域近十年之海水面變化速率研究 (A study on the sea level changing rate around Taiwan in the past ten years)，Institute of Transportation, MOTC. [in Mandarin]

Kuo, C. Y., Lin, L. C., Lan, W. H., Chuang, W. C., & Li, C. Y. (2015). 臺灣四周海域長期性之海水面變化趨勢評估 (A trend assessment of long-term sea level changes around Taiwan)，Institute of Transportation, MOTC.[in Mandarin]

Lin, H. J., Hsu, T. W., & Tseng, I. F. (2003). A Study on the Coastal Evolutions at Waisanding Barrier. Proceedings of the 25th Ocean Engineering Conference in Taiwan, Republic of China. Pp. 735-742. http://scholars.ntou.edu.tw/handle/123456789/14945. [in Mandarin]

Liu, W., Zhou, Z., Huang, W., Liu, H., & Young, C. (2018). Comparison of Historical and Synthetic Typhoons to Calculate Storm Surges under Different Return Periods for Predicting River Stages. Taiwan Water Conservancy, Vol. 66, No. 3. http://twc.bse.ntu.edu.tw/upload/ckfinder/files/1%E6%A0%A1-(10888)%E6%9F%B3%E6%96%87%E6%88%905%E4%BA%BA-p_1-17.pdf.

Liu, W. C. & Huang, W. C. (2020). Investigating typhoon-induced storm surge and waves in the coast of Taiwan using an integrally-coupled tide-surge-wave model. Ocean Engineering, Volume 212, 2020, Article 107571. https://doi.org/10.1016/j.oceaneng.2020.107571

Mäll M, Suursaar Ü, Nakamura R, Shibayama T (2017) Modelling a storm surge under future climate scenarios: case study of extratropical cyclone Gudrun (2005). Nat Hazards 89:1119–1144

Mäll M, Nakamura R, Suursaar Ü, Shibayama T (2020) Pseudo-climate modelling study on projected changes in extreme extratropical cyclones, storm waves and surges under CMIP5 multi-model ensemble: Baltic Sea perspective. Nat Hazards 102: 67-99. https://doi.org/10.1007/s11069-020-03911-2

Ministry of Culture. (2009). 西北颱 (Northwestern typhoon). LI, C. S. (Ed.), Encyclopedia of Taiwan. Ministry of Culture. http://nrch.culture.tw/twpedia.aspx?id=1036. Accessed 25 July 2021 [in Mandarin]

Ministry of Culture. (2009). Taiwan Strait. WANG, H. (Ed.), Encyclopedia of Taiwan. Ministry of Culture. https://nrch.culture.tw/twpedia.aspx?id=1459. [in Mandarin]

Mlawer, E. J., Taubman, S. J., Brown, P. D., Iacono, M. J., & Clough, S. A. (1997). Radiative transfer for inhomogeneous atmospheres: RRTM, a validated correlated–k model for the longwave. J. Geophys. Res., 102, 16663–16682. doi:10.1029/97JD00237

Nakamura, R., Shibayama, T., Esteban, M., Iwamoto, T., Nishizaki, S. (2020) Simulations of future typhoons and storm surges around Tokyo Bay using IPCC AR5 RCP 8.5 scenario in multi global climate models, Coastal Engineering Journal, 62(1), 101-127. https://doi.org/10.1080/21664250.2019.1709014

Nakamura, R., Mäll, M., & Shibayama, T. (2019). Street-scale storm surge load impact assessment using fine-resolution numerical modelling: a case study from Nemuro, Japan. Natural Hazards (2019) 99:391–422. https://doi.org/10.1007/s11069-019-03746-6

Nakamura, R., Shibayama, T., Esteban, M., & Iwamoto, T. (2016). Future typhoon and storm surges under different global warming scenarios: case study of typhoon Haiyan (2013). Nat Hazards (2016) 82:1645–1681. DOI 10.1007/s11069-016-2259-3

Nguyen, H. and Chen, Y. L. (2011). High-Resolution Initialization and Simulations of Typhoon Morakot (2009). Monthly Weather Review - MON WEATHER REV. 139. 1463-1491. 10.1175/2011MWR3505.1

Niu, G. Y., Yang, Z. L., Mitchell, K. E., Chen, F., Ek, M. B., Barlage, M., Kumar, A., Manning, K., Niyogi, D., Rosero, E., Tewari, M., & Xia, Y. (2011). The community Noah land surface model with multiparameterization options (Noah–MP): 1. Model description and evaluation with local–scale measurements. J. Geophys. Res., 116, D12109. doi:10.1029/2010JD015139

Ocean Data Bank (ODB) of the Ministry of Science and Technology, Republic of China. http://www.odb.ntu.edu.tw/. Accessed 25 July 2021.

Peng, H. Y., Tseng, K. H., Chien, H., & Chen, Y. D. (2019). Utilizing Multitemporal Satellite Images to Investigate Topographical Changes of Waisanding Sandbar. Taiwan Journal of Geoinfomatics, 7(2), 103-119. http://www.mporg.tw/files/WaisandingSandbar.pdf. [in Mandarin]

Sato, T., F. Kimura, and A. Kitoh. 2007. Projection of Global Warming onto Regional Precipitation over Mongolia Using a Regional Climate Model. Journal of Hydrology 333 (1): 144–154. doi:10.1016/j.jhydrol.2006.07.023.

Schär, C., C. Frei, D. Lüthi, and H. C. Davies. 1996. Surrogate Climate-Change Scenarios for Regional Climate Models. Geophysical Research Letter 23: 669–672. doi:10.1029/96GL00265.

Skamarock, W. C., Klemp, J. B., Dudhia, J., Gill, D. O., Barker, D., Duda, M. G., … Powers, J. G. (2008). A Description of the Advanced Research WRF Version 3 (No. NCAR/TN-475+STR). University Corporation for Atmospheric Research. doi:10.5065/D68S4MVH

Tseng, Y. H., Breaker, C. L., & Chang, T. Y. (2010). Sea level variations in the regional seas around Taiwan, Journal of Oceanography, 66, 27-39.

Walsh, K. J. E., Camargo, S. J., Knutson, T. R., Kossin, J., Lee, T. C., Murakami, H., & Patricola, C. (2019). Tropical cyclones and climate change. Tropical Cyclone Research and Review. Volume 8, Issue 4, Pages 240-250. ISSN 2225-6032. https://doi.org/10.1016/j.tcrr.2020.01.004

Wang, S., S. J. Camargo, A. H. Sobel, and L. M. Polvani. 2014. Impact of the Tropopause Temperature on the Intensity of Tropical Cyclones-an Idealized Study Using a Mesoscale Model. Journal of Atmospheric Science 71 (11): 4333–4348. doi:10.1175/JAS-D-14-0029.1.

Wang, H., Long, L., Kumar, A., Wang, W., Schemm, J. E., Zhao, M., Vecchi, G. A., Larow, T. E., Lim, Y., Schubert, S. D., Shaevitz, D. A., Camargo, S. J., Henderson, N., Kim, D., Jonas, J. A., & Walsh, K. J. E. (2014). How Well Do Global Climate Models Simulate the Variability of Atlantic Tropical Cyclones Associated with ENSO?, Journal of Climate, 27(15), 5673-5692. Retrieved Aug 9, 2021, from https://journals.ametsoc.org/view/journals/clim/27/15/jcli-d-13-00625.1.xml

Yang, P., Doong, D., & Chen, Y. (2018). Long-term analysis on Storm Surge in Taiwan Coastal Ocean. Proceedings of the 40th Ocean Engineering Conference in Taiwan, Kaohsiung, Taiwan. http://www.tsoe.org.tw/downloads/thesis/2018A801.pdf. [in Mandarin]

Yang, Z. L., Niu, G. Y., Mitchell, K. E., Chen, F., Ek, M. B., Barlage, M., Longuevergne, L., Manning, K., Niyogi, D., Tewari, M., & Xia, Y. (2011). The community Noah land surface model with multiparameterization options (Noah–MP): 2. Evaluation over global river basins. J. Geophys. Res., 116, D12110. doi:10.1029/2010JD015140

Yu, Y. C., Chen, H., Shih, H. J., Chang, C. H., Hsiao, S. C., Chen, W. B., Chen, Y. M., Su, W. R., & Lin, L. Y. (2019). Assessing the Potential Highest Storm Tide Hazard in Taiwan Based on 40-Year Historical Typhoon Surge Hindcasting. Atmosphere 2019, 10, 346, doi:10.3390/atmos10060346

Zappa G, Shaffrey LC, Hodges KI, Sansom PG, Stephenson DB (2013b) A multi-model assessment of future projections of north atlantic and european extratropical cyclones in the CMIP5 climate models. J Climate 26:5846–5862.

Supplementary information

1. Bathymetry in case study area

The bathymetry data from the ODB had a resolution of 0.002°, which is around 200 m in grid size. Due to issues relating to the accuracy of satellite images and the presence of constantly shifting sandbars along the coastline, some modifications were made to the SRTM3 coastline data to match the bathymetry data provided by the ODB to avoid errors in simulations caused by the mismatch between two data sources. This modified mesh is shown in Figure A1.
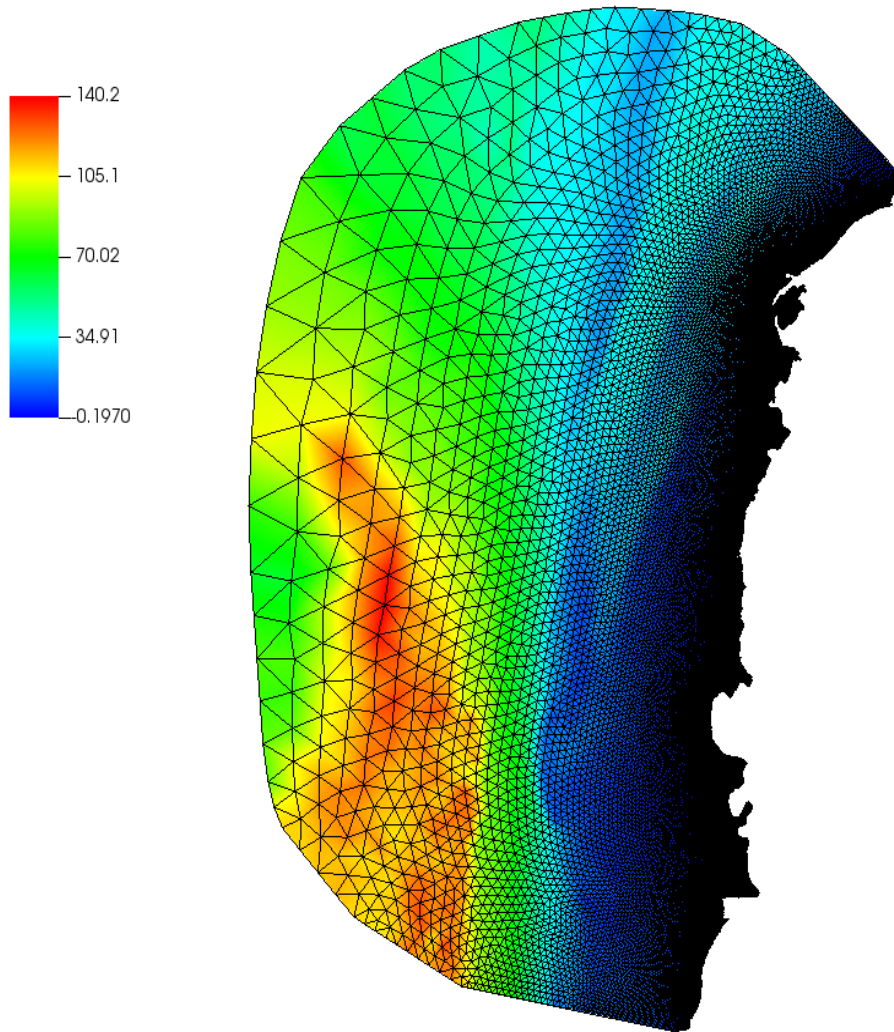

Figure A1: FVCOM mesh, showing water depth (unit: m).

2. List of GCMs used in the model

Table A: GCM ensemble list used in the present simulations (after Mall et al., 2020)

Model name	Model institution	Atmospheric resolution		Ensemble number	Ensemble name
		Horizontal	Vertical levels		
ACCESS1-0	Commonwealth Scientific and Industrial Research Organization	192×145 (N96)	38	1	r1i1p1
ACCESS1-3	(CSIRO) and Bureau of Meteorology (BOM), Australia			1	r1i1p1
BCC-CSM1-1-m	Beijing Climate Center, China Meteorological Administration	T106	26	1	r1i1p1
CCSM4	National Center for Atmospheric Research	0.9°×1.25°	27	6	r1i1p1, r2i1p1, r3i1p1, r4i1p1, r5i1p1, r6i1p1
CESM1-BGC				1	r1i1p1
CESM1-CAM5	NFS-DOE-NCAR	0.9°×1.25°	27	3	r1i1p1, r2i1p1, r3i1p1
CMCC-CM	Centre Euro-Miditerraneo per I Cambiamenti Climatici	0.75×0.75 (T159)	31	1	r1i1p1
EC-EARTH	EC-EARTH consortium	1.125 long. Spacing, T159L62	62	4	r1i1p1, r6i1p1, r8i1p1, r12i1p1
GISS-E2-H-CC	NASA Goddard Institute for Space Studies	Nominally 1°	40	1	r1i1p1
GISS-E2-R-CC				1	r1i1p1
HadGEM2-AO	National Institute of Meteorological Research/Korea Meteorological Administration	1.875 long×1.25 lat (N96)	60	1	r1i1p1
HadGEM2-CC	UK Met Office Hadley Centre (additional HadGEM2-ES	1.875 long×1.25 lat (N96)	60	3	r1i1p1, r2i1p1, r3i1p1
HadGEM2-ES	realizations contributed by Instituto Nacional de Pesquisas Espaciais)		38	4	r1i1p1, r2i1p1, r3i1p1, r4i1p1
MRI-CGCM3	Meteorological Research Institute	320×160 (TL159)	48	1	r1i1p1

3. Changes in SST, AAT and RH for global warming scenarios.

Figure A1 shows the changes in SST for two different time horizons, 2041~2060 and 2081~2100, for both pathways by modifying the observed SST in CFSv2 data at 00:00 UTC on August 7th, 2015. Figures A2 and A3 show the changes in AAT and RH for the two time horizons, respectively.
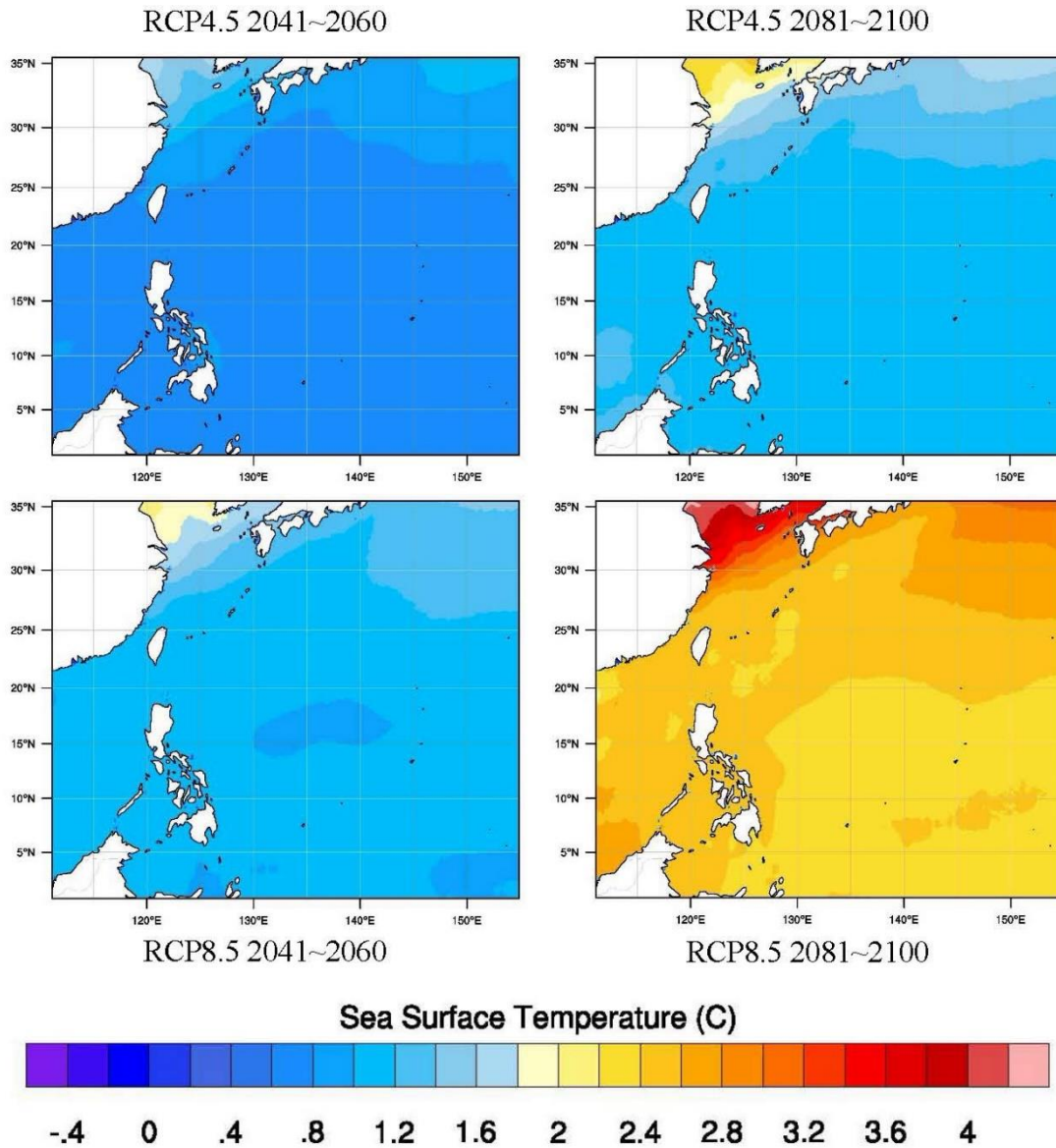

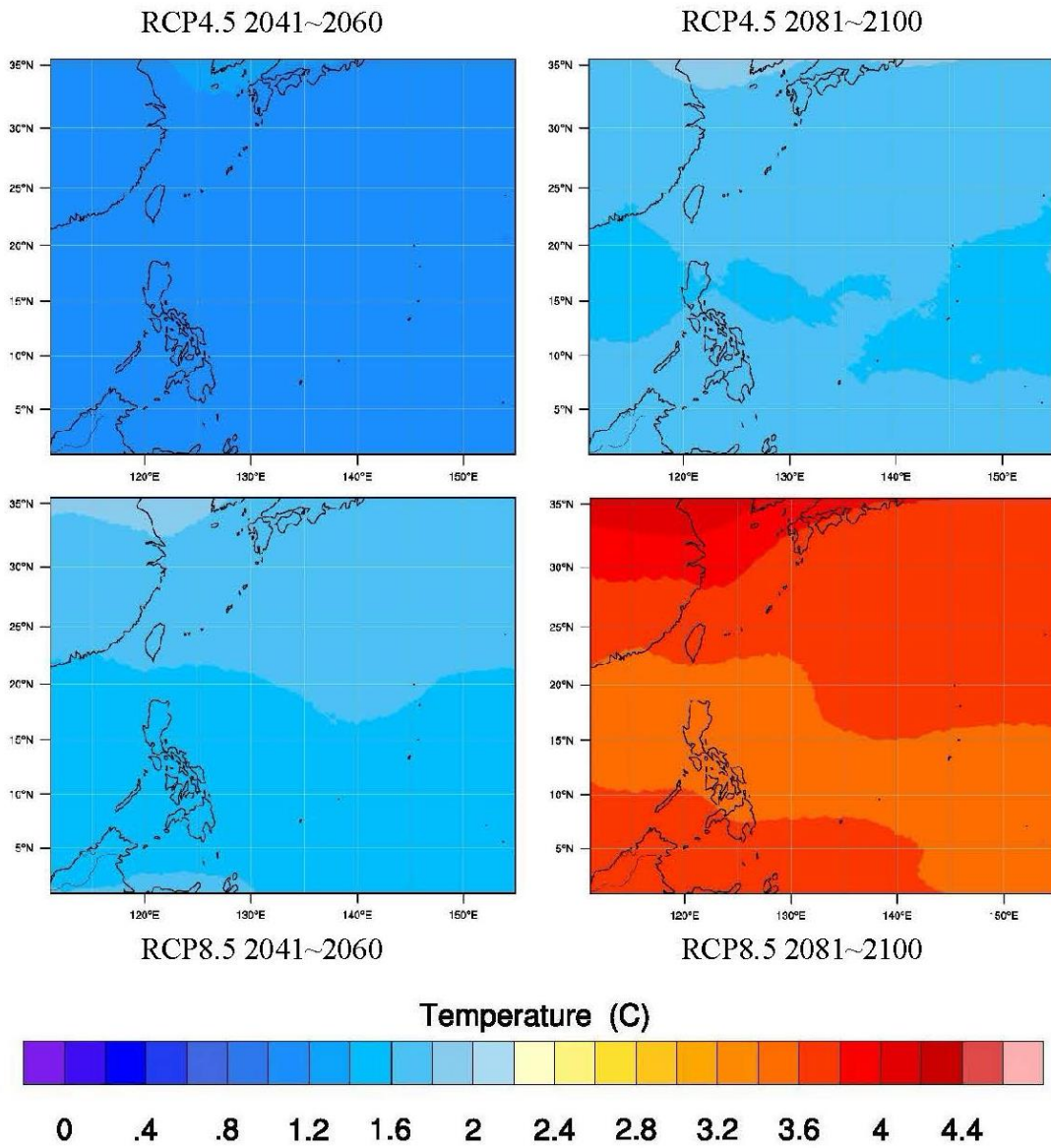Figure A1: SST under different future scenarios and time horizons

RCP4.5 2041~2060   RCP4.5 2081~2100

RCP8.5 2041~2060   RCP8.5 2081~2100

Temperature (C)

0   .4   .8   1.2   1.6   2   2.4   2.8   3.2   3.6   4   4.4

Figure A2: AAT under different future scenarios and time horizons

RCP4.5 2041~2060   RCP4.5 2081~2100

RCP8.5 2041~2060   RCP8.5 2081~2100

Relative Humidity (%)

-7   -6   -5   -4   -3   -2   -1   0   1   2   3
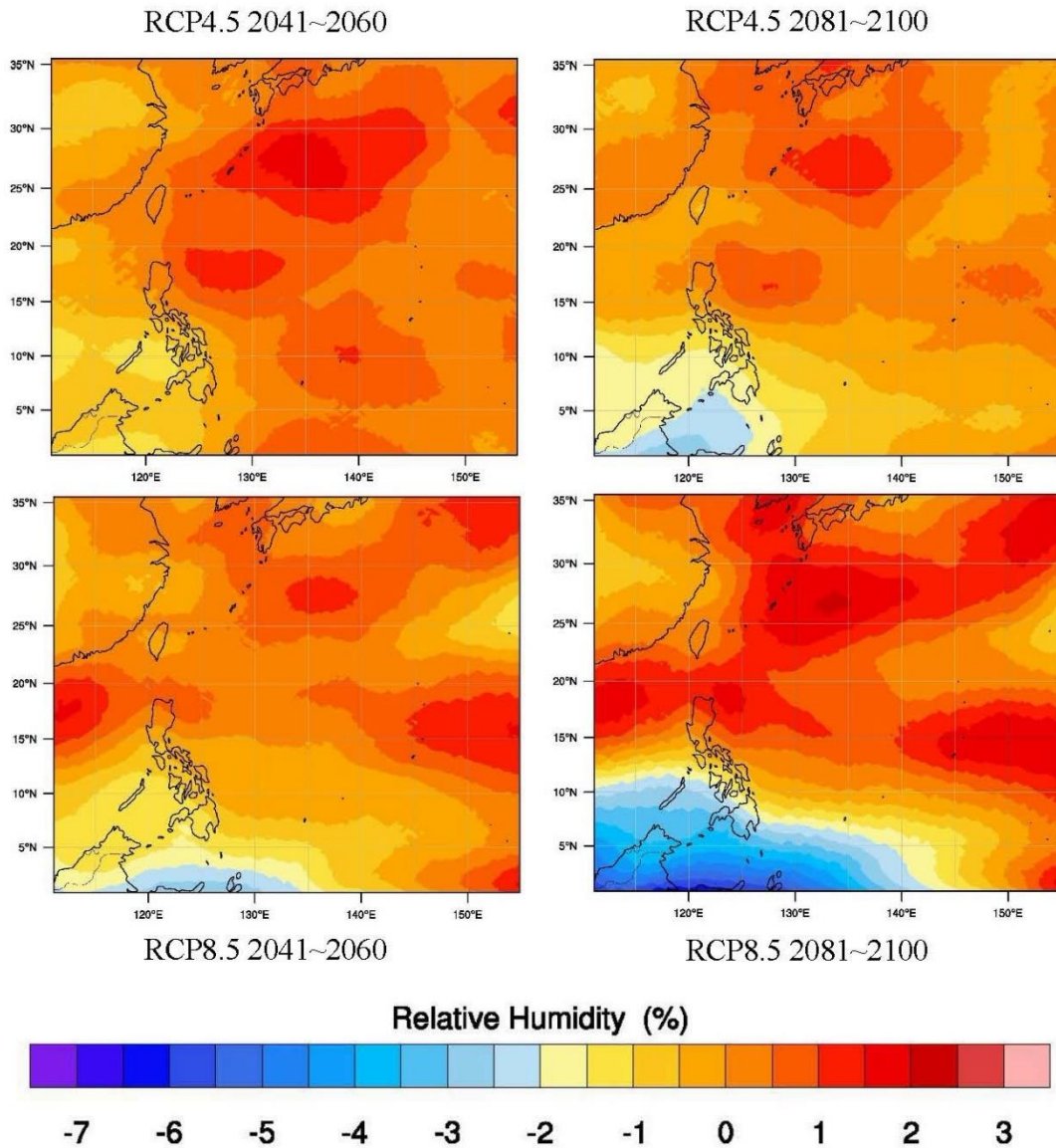
Figure A3: RH under different future scenarios and time horizons

4. Wind fields for various scenarios

The wind fields simulated for the RCP8.5 2081~2100 time horizon over Taiwan are shown in Figure A4. Figure A5 and A6 shows the wind fields in the simulation domain under two different future scenarios while the typhoon is closest to the study area.
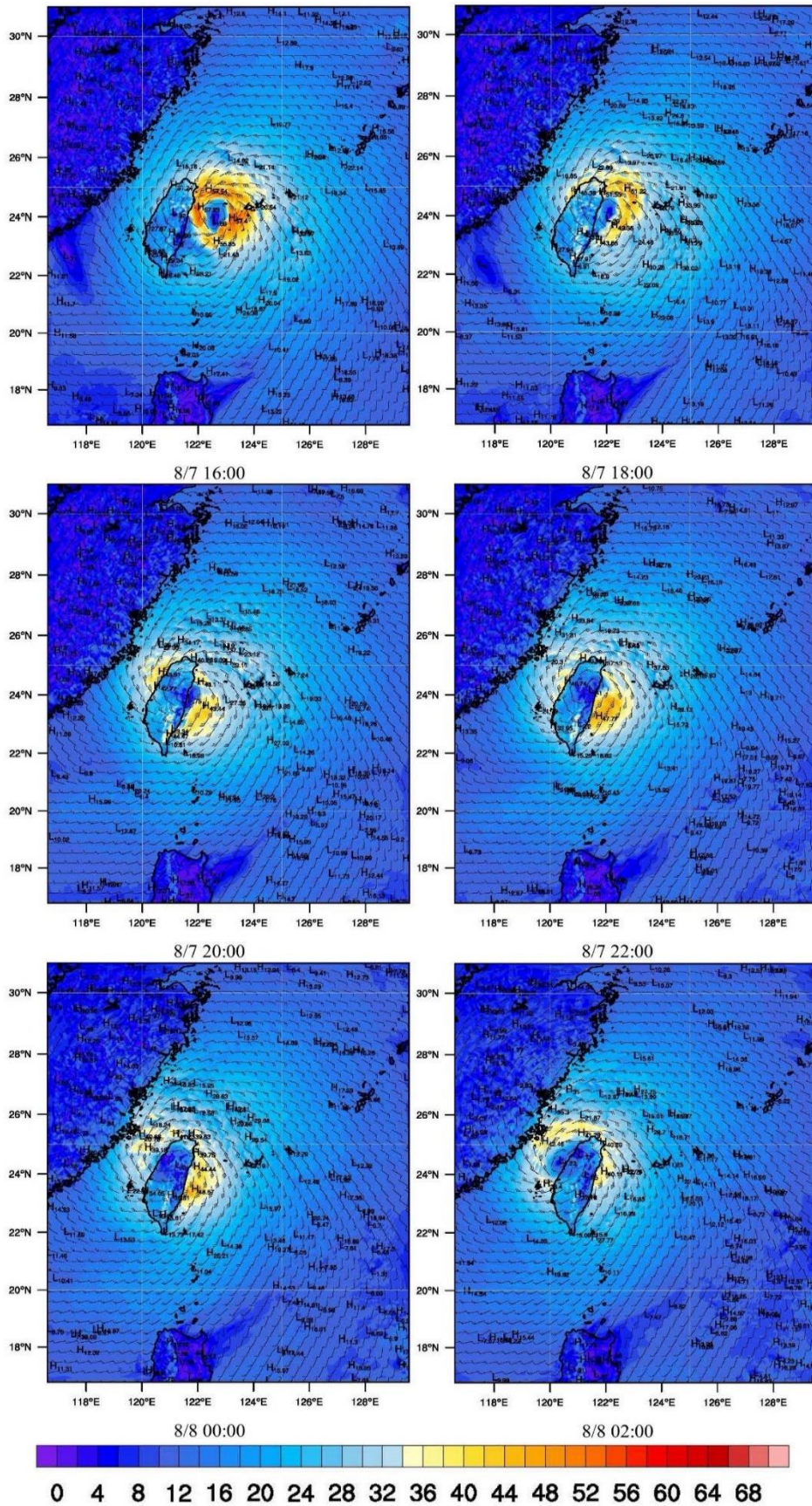
Figure A4: Wind field of Typhoon Soudelor simulated for the RCP8.5 2081~2100 time horizon (unit: m/s)
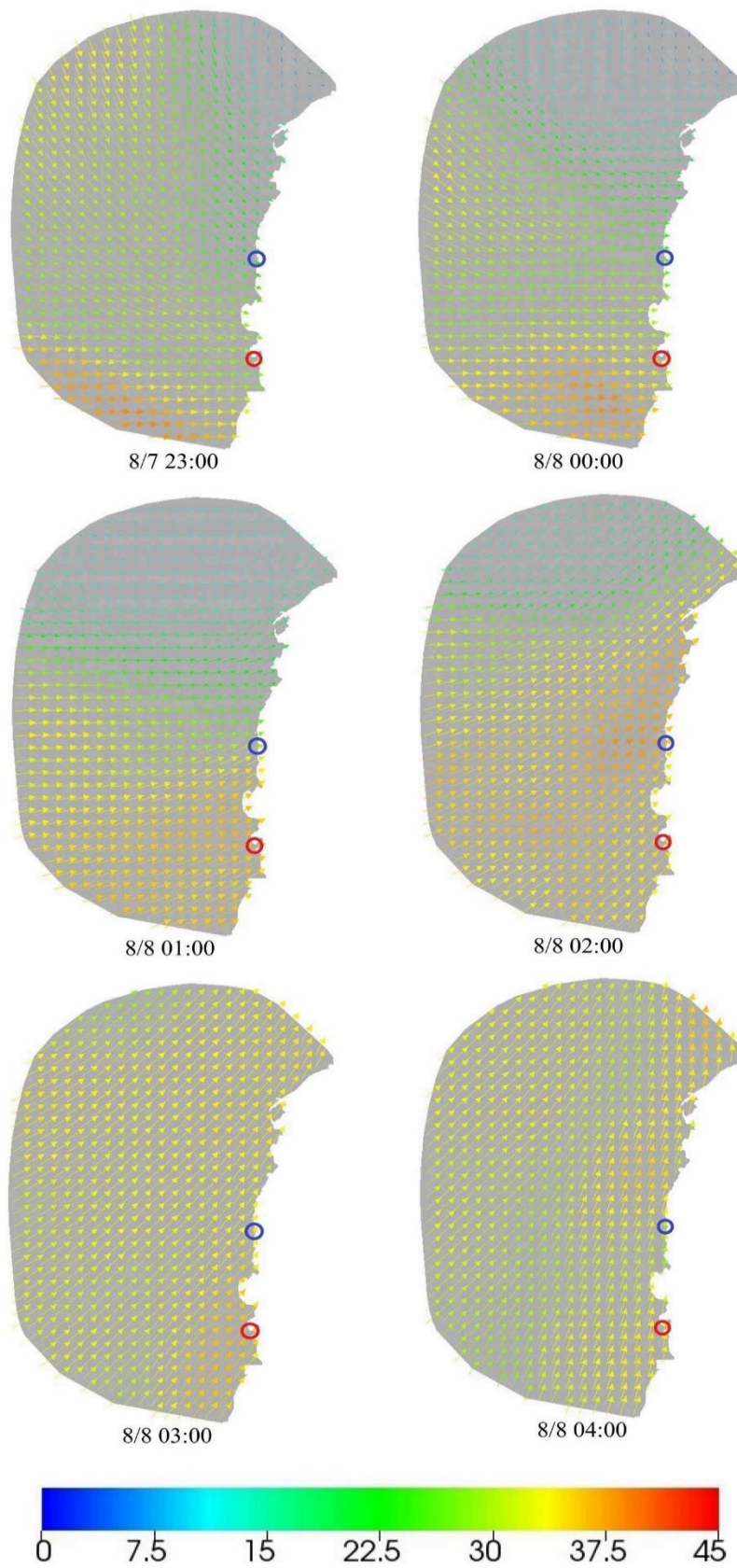
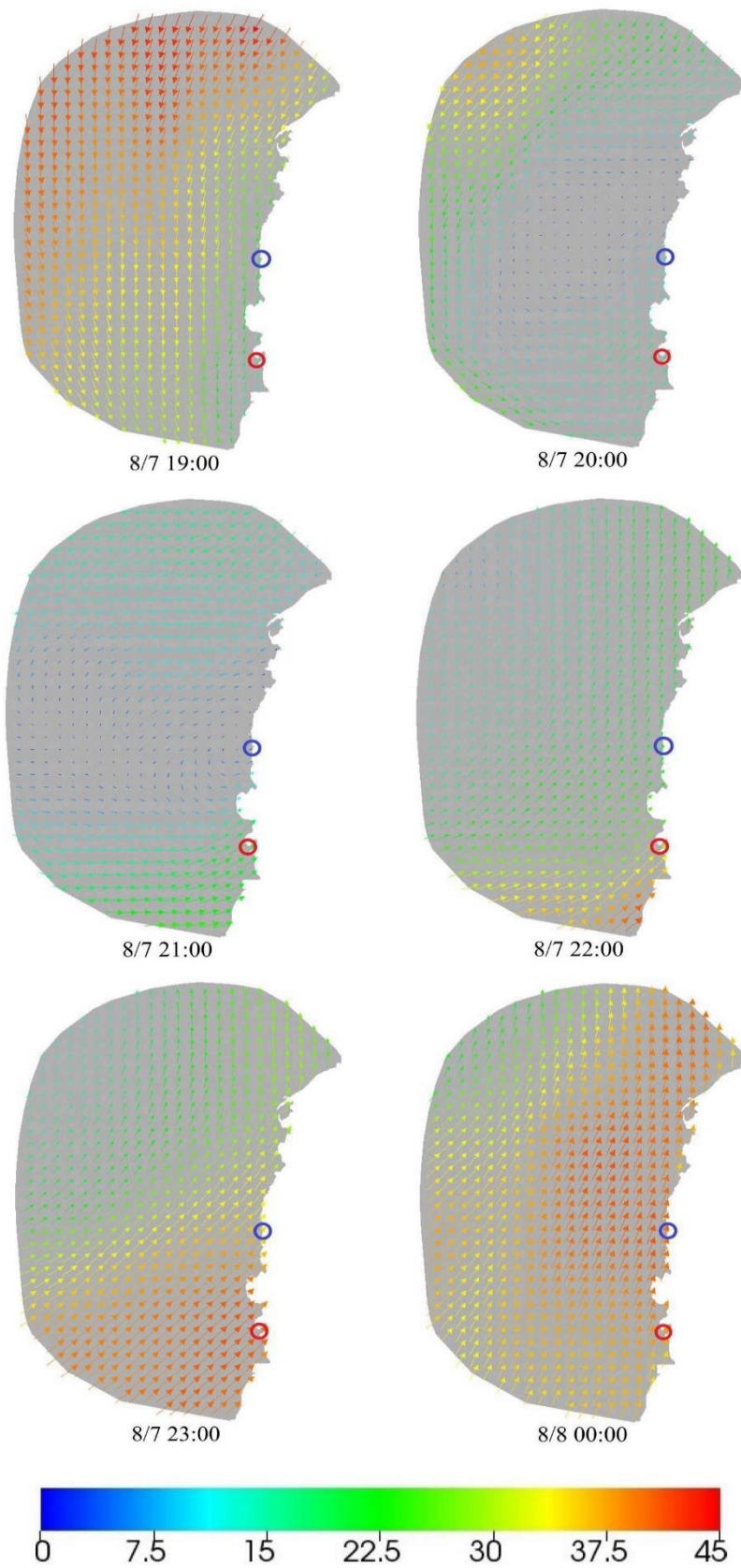Figure A5: Wind field in FVCOM forcing files under RCP8.5 2041~2060 scenario (unit:m/s)

Figure A6: Wind field in FVCOM forcing files under RCP8.5 2081~2100 scenario (unit:m/s)